Institute of Cosmophysical Research and Radio Wave Propagation FEB RAS

Hybrid methods for analyzing natural data in space weather forecasting problems

Subject of research

Creation of geophysical data analysis methods aimed at studying processes in near-Earth space and detecting space weather anomalies

- ***Modeling and analysis of ionospheric parameters (based on ionosonde data)***
- ***Modeling and analysis of cosmic ray intensity variations data (based on neutron monitor data)***
- ***Study of geomagnetic field variations during disturbed periods (according to magnetometer data)***

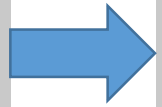

Automated methods for data analysis and rapid detection of anomalous manifestations of space weather

Approach used

System analysis

Regular component
(calm periods in NES)
Parametric model

- ***Classical methods and approaches***
- ***Nonlinear approximation schemes***
- ***Artificial intelligence***

Anomalous component
(disturbed periods)
Nonparametric approach

- ***Nonlinear approximation schemes***
- ***Artificial intelligence***

Flexible mathematical structures + Adaptive methods

Adequate data description models

Deeper study of physical processes and interactions between objects

Generalized multicomponent model of ionospheric parameters (GMCM)

$$f(t) = A^{REG}(t) + U(t) + e(t) = \sum_{\mu=\overline{1,T}} \sum_{j} G_j^{\mu} \alpha_j^{\mu}(t) + \sum_{i,\eta} \beta_{i,\eta}^{dist}(t) + e(t)$$

$$= \sum_{\mu=\overline{1,T}} \sum_{k=\overline{1,N_{j^{reg}}^{\mu}}} s_{j^{reg},k}^{\mu} b_{j^{reg},k}^{\mu}(t) + \sum_{i=\overline{1,3}} \sum_{\eta,n} P_{i,\eta}^{ad}(d_{\eta,n}) \Psi_{\eta,n}(t) + e(t)$$

Nadezhda Fetisova

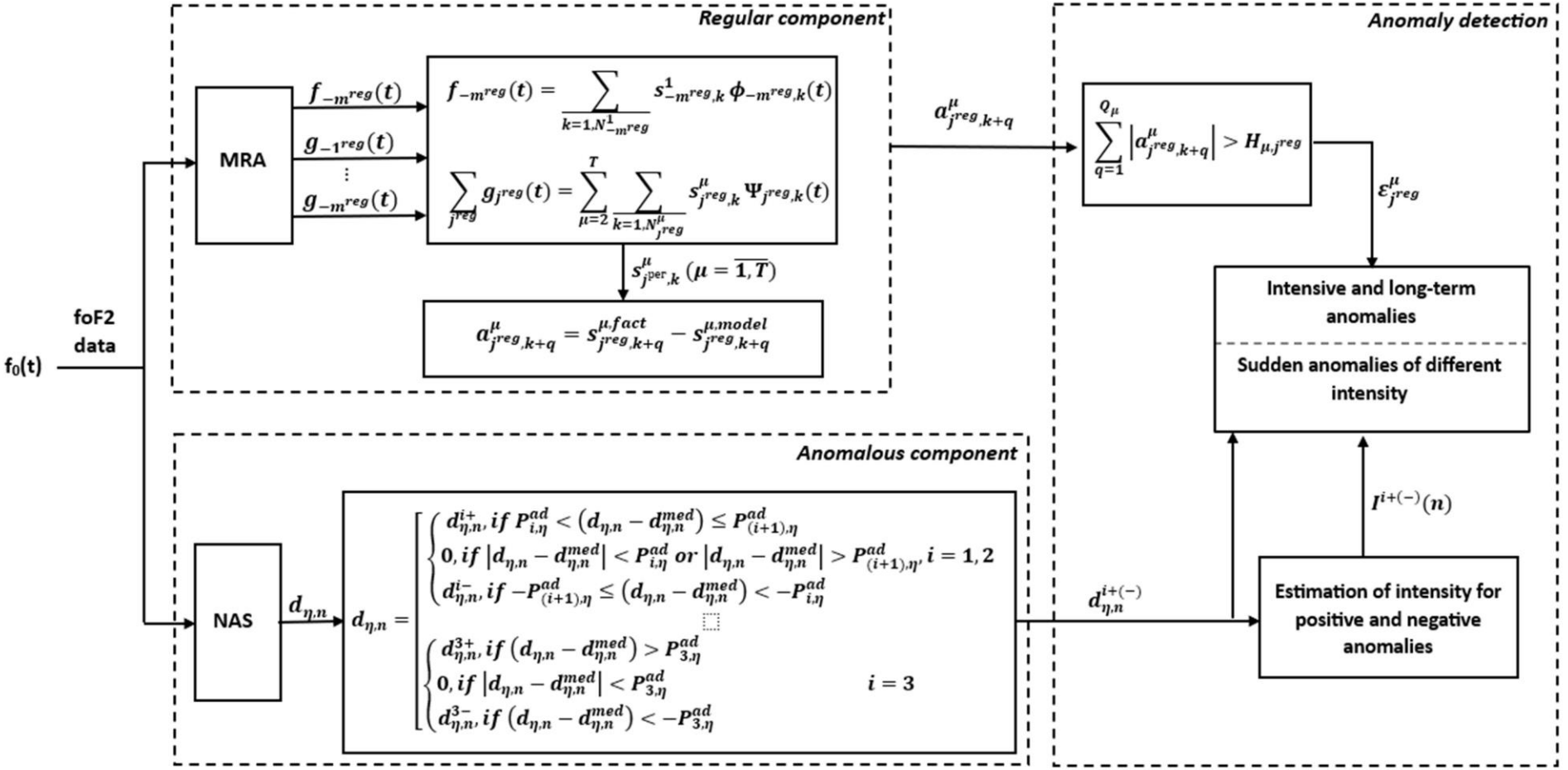

GMCM identification

1. Multiresolution wavelet analysis

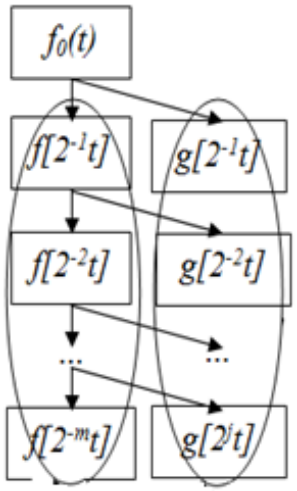

$$f(t) = f_{-m}(t) + \sum_{j=-1}^{-m} g_j(t)$$

2. ARIMA models

Parameter estimation

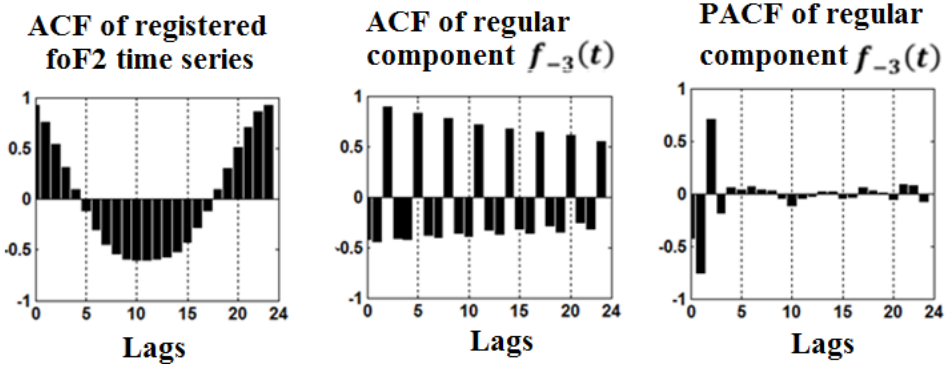

GMCM regular component (regular time variations of ionospheric parameters)

$$A^{REG}(t) = f_{-m^{reg}}(t) + \sum_{j^{reg}} g_{j^{reg}}(t) = \sum_{\mu=\overline{1,T}} \sum_{k=1,\dots,N^{\mu}_{j^{reg}}} s^{\mu}_{j^{reg},k} b^{\mu}_{j^{reg},k}(t)$$

$$s^{\mu}_{j^{reg},k} = \sum_{l=1}^{p^{\mu}_{j^{reg}}} \gamma^{\mu}_{j^{reg},l} \omega^{\mu}_{j^{reg},k-l}(t) - \sum_{n=1}^{h^{\mu}_{j^{reg}}} \theta^{\mu}_{j^{reg},n} a^{\mu}_{j^{reg},k-n}(t)$$

Modeling of foF2 during quiet ionosphere

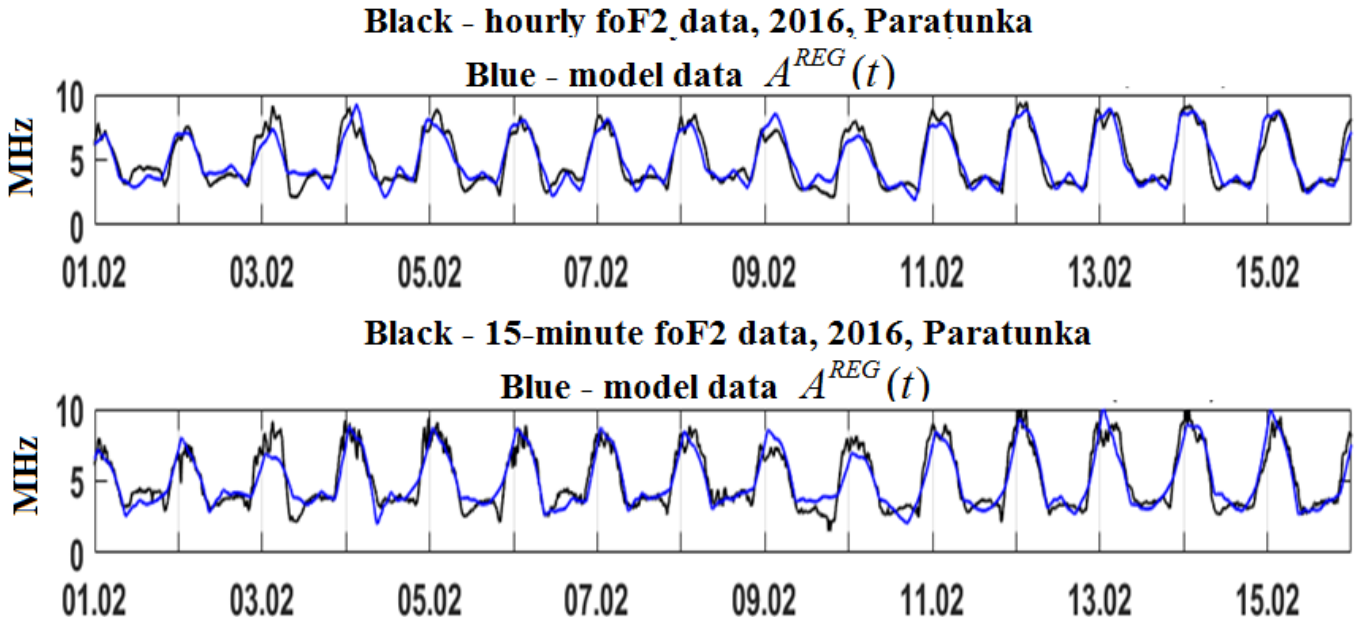

GMCM anomalous component

Nonlinear approximating schemes in wavelet basis

$$U(t) = \sum_{i,\eta} \beta_{i,\eta}^{dist}(t) = \sum_{i=\overline{1,3}} \sum_{\eta,n} P_{i,\eta}(d_{\eta,n}) \Psi_{\eta,n}(t)$$

$\{\Psi_{\eta,n}\}_{\eta,n \epsilon Z}$ *is wavelet*

$$P_{1,\eta}(d_{\eta,n}) = \begin{cases} 0, \text{if } |d_{\eta,n}| \le T_{1,\eta} \text{ or } |d_{\eta,n}| > T_{2,\eta} \\ d_{\eta,n}, \text{if } T_{1,n} < |d_{\eta,n}| \le T_{2,\eta} \end{cases}$$

$$P_{2,\eta}(d_{\eta,n}) = \begin{cases} 0, \text{if } |d_{\eta,n}| \le T_{2,\eta} \text{ or } |d_{\eta,n}| > T_{3,\eta} \\ d_{\eta,n}, \text{if } T_{2,\eta} < |d_{\eta,n}| \le T_{3,\eta} \end{cases}$$

$$P_{3,\eta}(d_{\eta,n}) = \begin{cases} 0, \text{if } |d_{\eta,n}| \le T_{3,\eta} \\ d_{\eta,n}, \text{if } |d_{\eta,n}| > T_{3,\eta} \end{cases}$$

$T_{1,\eta}, T_{2,\eta}, T_{3,\eta}$ are thresholds determining anomalies on the scale η of weak ***(class 1)***, moderate ***(class 2)*** and strong ***(class 3)*** intensity

Adaptive thresholds:

$P_{i,\eta}^{a\partial}, i = \overline{1,3}$

Detection of short-period anomalous changes of different intensity and duration

Anomalies of weak intensity (class 1)

Anomalies of moderate intensity (class 2)

Anomalies of strong intensity (class 3)

$$d_{\eta,n} = \begin{cases} d_{\eta,n}^{1+}, if \ P_{1,\eta}^{ad} < \left(d_{\eta,n} - d_{\eta,n}^{med}\right) \le P_{2,\eta}^{ad} \\ 0, \ if \ \left|d_{\eta,n} - d_{\eta,n}^{med}\right| < P_{1,\eta}^{ad} \ or \ \left|d_{\eta,n} - d_{\eta,n}^{med}\right| > P_{2,\eta}^{ad} \\ d_{\eta,n}^{1-}, if -P_{2,\eta}^{ad} \le \left(d_{\eta,n} - d_{\eta,n}^{med}\right) < -P_{1,\eta}^{ad} \\ d_{\eta,n}^{2+}, if \ P_{2,\eta}^{ad} < \left(d_{\eta,n} - d_{\eta,n}^{med}\right) \le P_{3,\eta}^{ad} \\ 0, \ if \ \left|d_{\eta,n} - d_{\eta,n}^{med}\right| < P_{2,\eta}^{ad} \ or \ \left|d_{\eta,n} - d_{\eta,n}^{med}\right| > P_{3,\eta}^{ad}, \\ d_{\eta,n}^{2-}, if -P_{3,\eta}^{ad} \le \left(d_{\eta,n} - d_{\eta,n}^{med}\right) < -P_{2,\eta}^{ad} \\ d_{\eta,n}^{3+}, if \left(d_{\eta,n} - d_{\eta,n}^{med}\right) > P_{3,\eta}^{ad} \\ 0, \ if \ \left|d_{\eta,n} - d_{\eta,n}^{med}\right| < P_{3,\eta}^{ad} \\ d_{\eta,n}^{3-}, if \left(d_{\eta,n} - d_{\eta,n}^{med}\right) < -P_{3,\eta}^{ad} \end{cases}$$

$$P_{i,\eta}^{\text{ad}} = V_i * St_\eta, \quad St_\eta = \sqrt{\frac{1}{\Phi - 1} \sum_{n=1}^{\Phi} \left(d_{\eta,n} - \overline{d_{\eta,n}}\right)^2},$$

Φ is the length of a moving time window

V_i is the threshold coefficient.

Intensity estimation

Intensity of each class *i*: $I^{i+(-)}(n) = \sum_\eta \left|d_{\eta,n}^{i+(-)}\right|,$

General intensity: $I^{+(-)}(n) = \sum_\eta \left|d_{\eta,n}^{+(-)}\right|.$

Detection of intense ionospheric anomalies

Algorithm for detecting intense anomalies

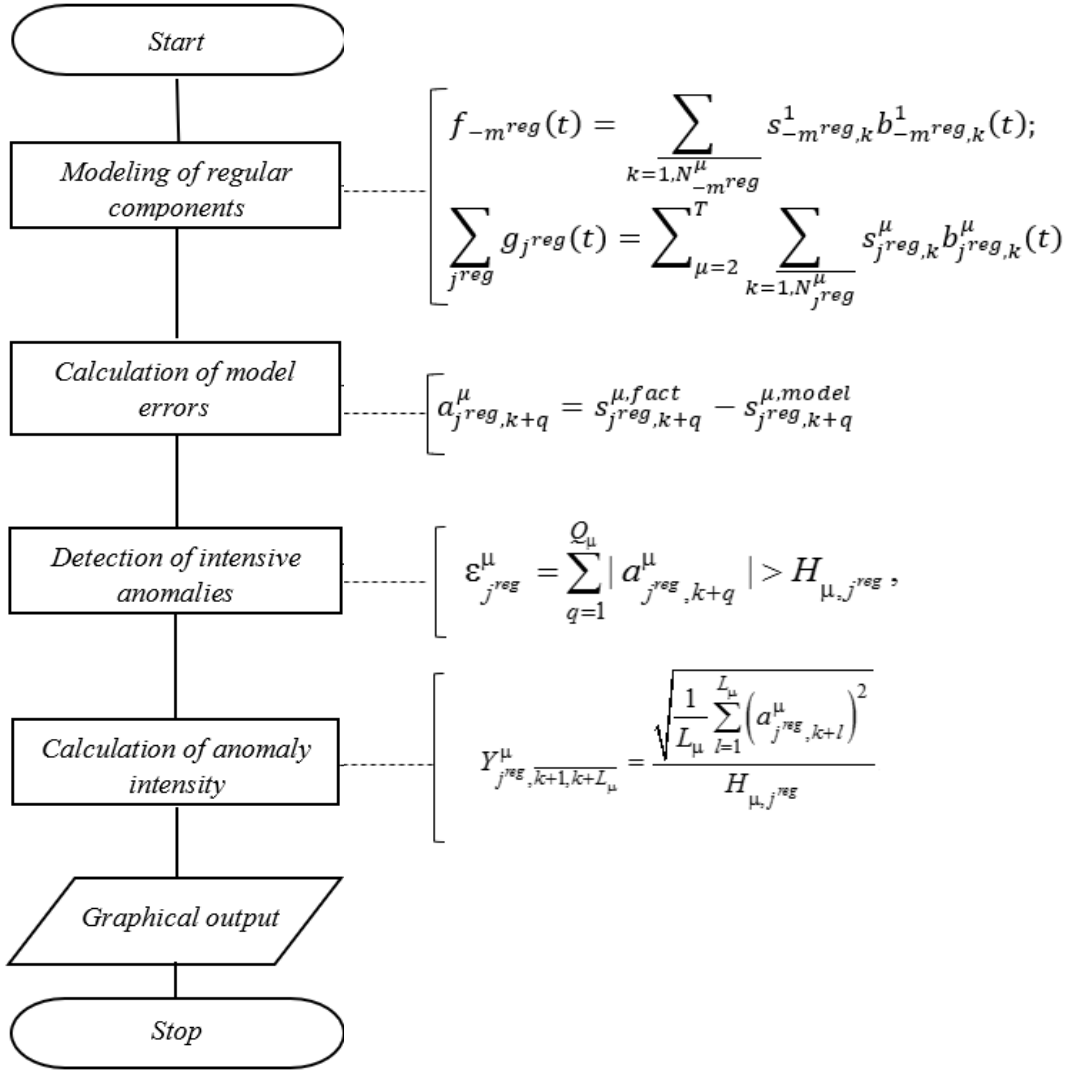

$$f_{-m^{reg}}(t) = \sum_{k=1,N^{\mu}_{-m^{reg}}} s^{1}_{-m^{reg},k} b^{1}_{-m^{reg},k}(t);$$

$$\sum_{j^{reg}} g_{j^{reg}}(t) = \sum_{\mu=2}^{T} \sum_{k=1,N^{\mu}_{j^{reg}}} s^{\mu}_{j^{reg},k} b^{\mu}_{j^{reg},k}(t)$$

$$a^{\mu}_{j^{reg},k+q} = s^{\mu,fact}_{j^{reg},k+q} - s^{\mu,model}_{j^{reg},k+q}$$

$$\varepsilon^{\mu}_{j^{reg}} = \sum_{q=1}^{Q_{\mu}} | a^{\mu}_{j^{reg},k+q} | > H_{\mu,j^{reg}},$$

$$Y^{\mu}_{j^{reg},\overline{k+1,k+L_{\mu}}} = \frac{\sqrt{\frac{1}{L_{\mu}} \sum_{l=1}^{L_{\mu}} \left(a^{\mu}_{j^{reg},k+l} \right)^2}}{H_{\mu,j^{reg}}}$$

Application of the algorithm

Ionospheric data analysis (Paratunka station) during the magnetic storm on March 17, 2015

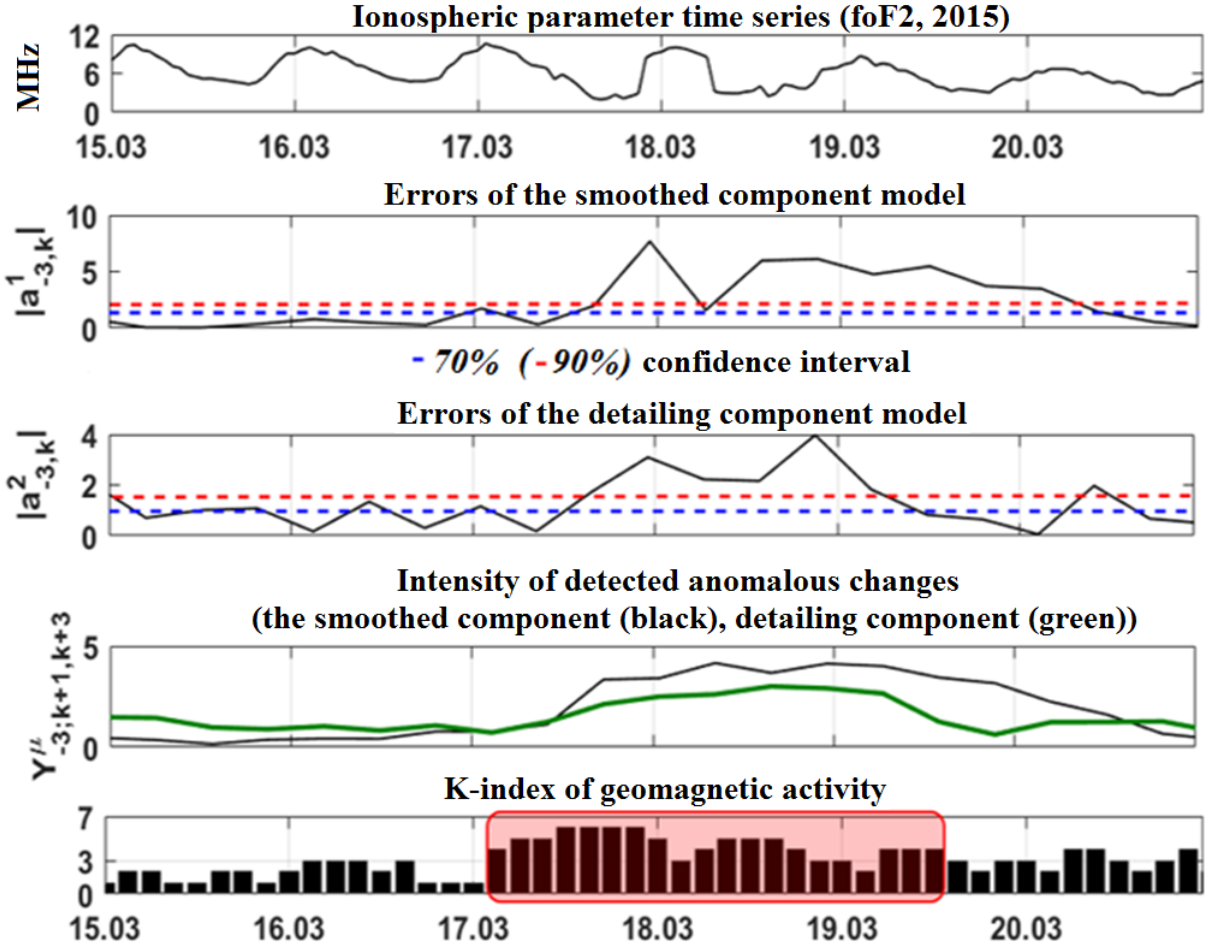

– the threshold $H_{\mu,-3}$ (70% confidence interval)

– the threshold $H_{\mu,-3}$ (90% confidence interval)

Detection of sudden ionospheric anomalies

Algorithm for recognizing sudden anomalies of different intensity

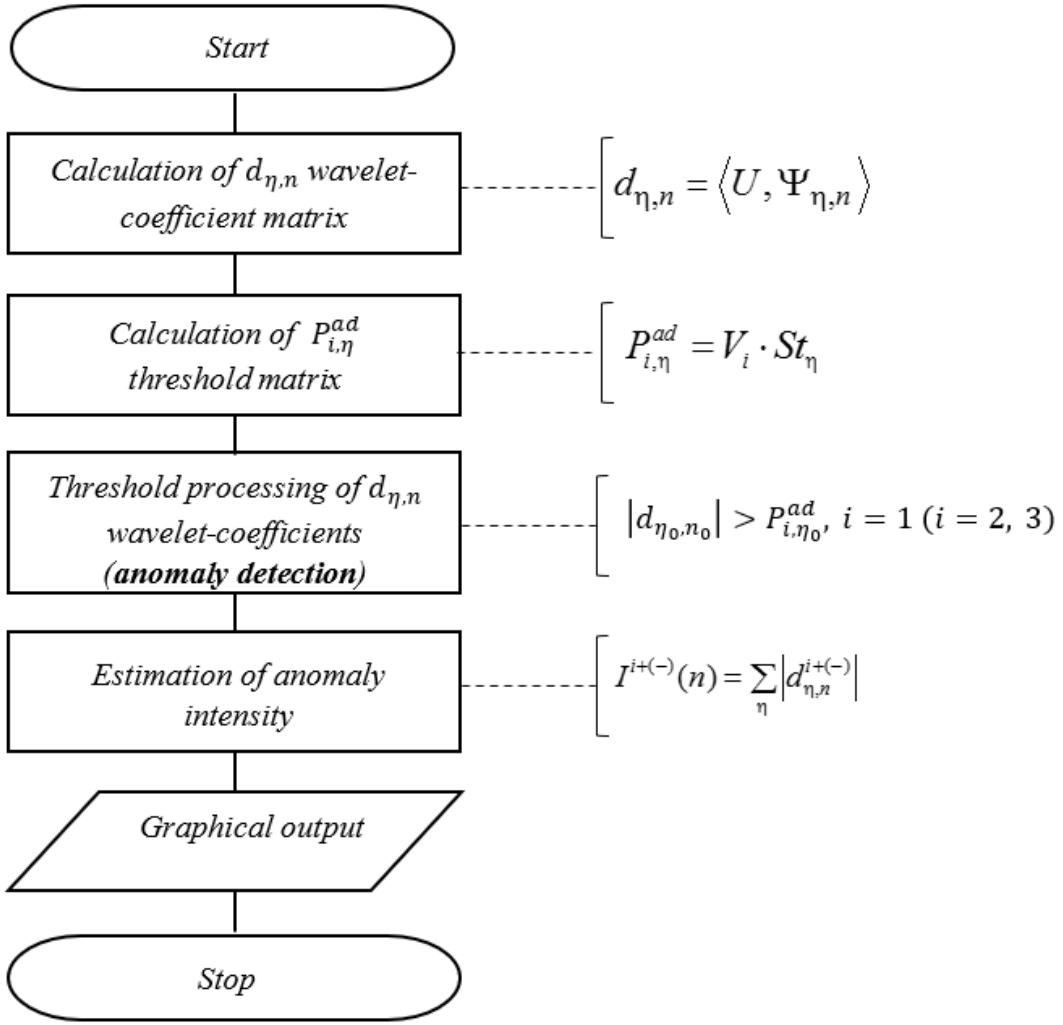

Application of the algorithm

Ionospheric data analysis (Paratunka station) during the magnetic storm on August 25, 2018

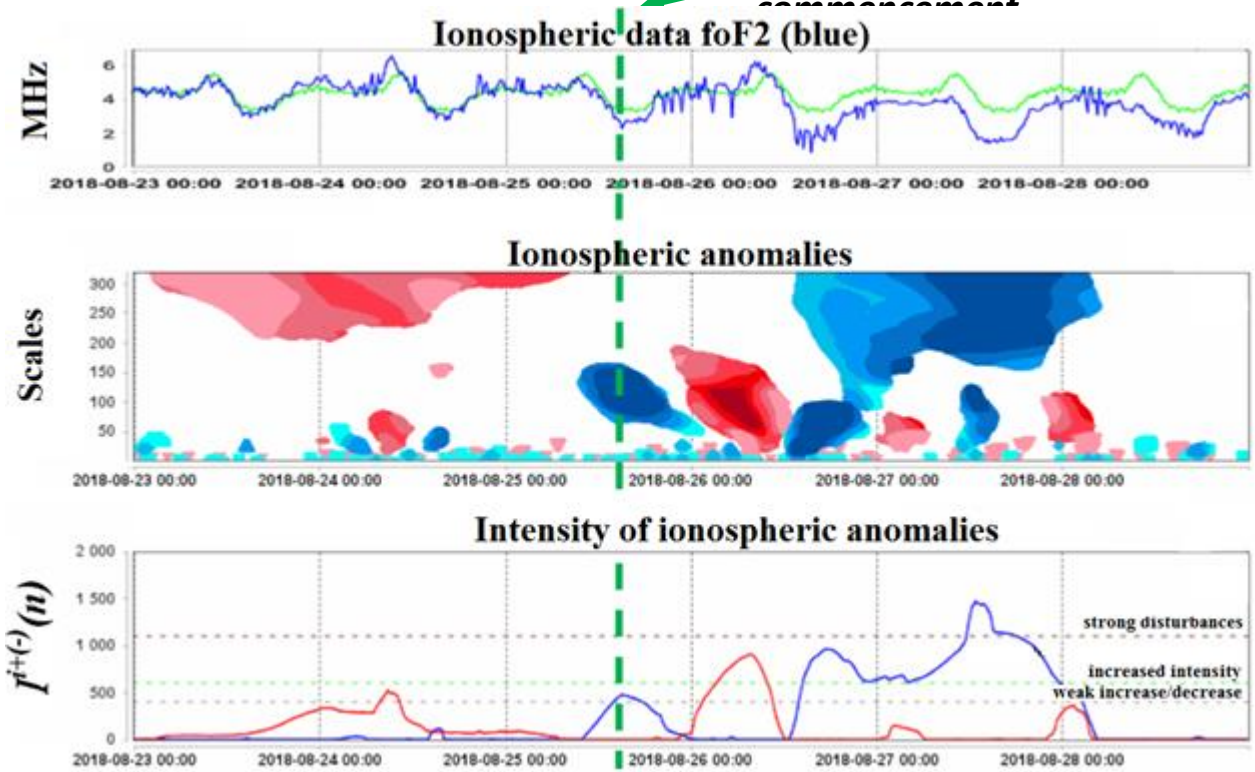

Anomalies of weak intensity (class 1)

$400 < I^{+(-)}(n) < 600$

Anomalies of moderate intensity (class 2)

$600 < I^{+(-)}(n) \leq 1100$

Anomalies of strong intensity (class 3)

$I^{+(-)}(n) > 1100$

Modeling of foF2 time variations based on NARX networks and threshold wavelet filtering

Yurii Polozov

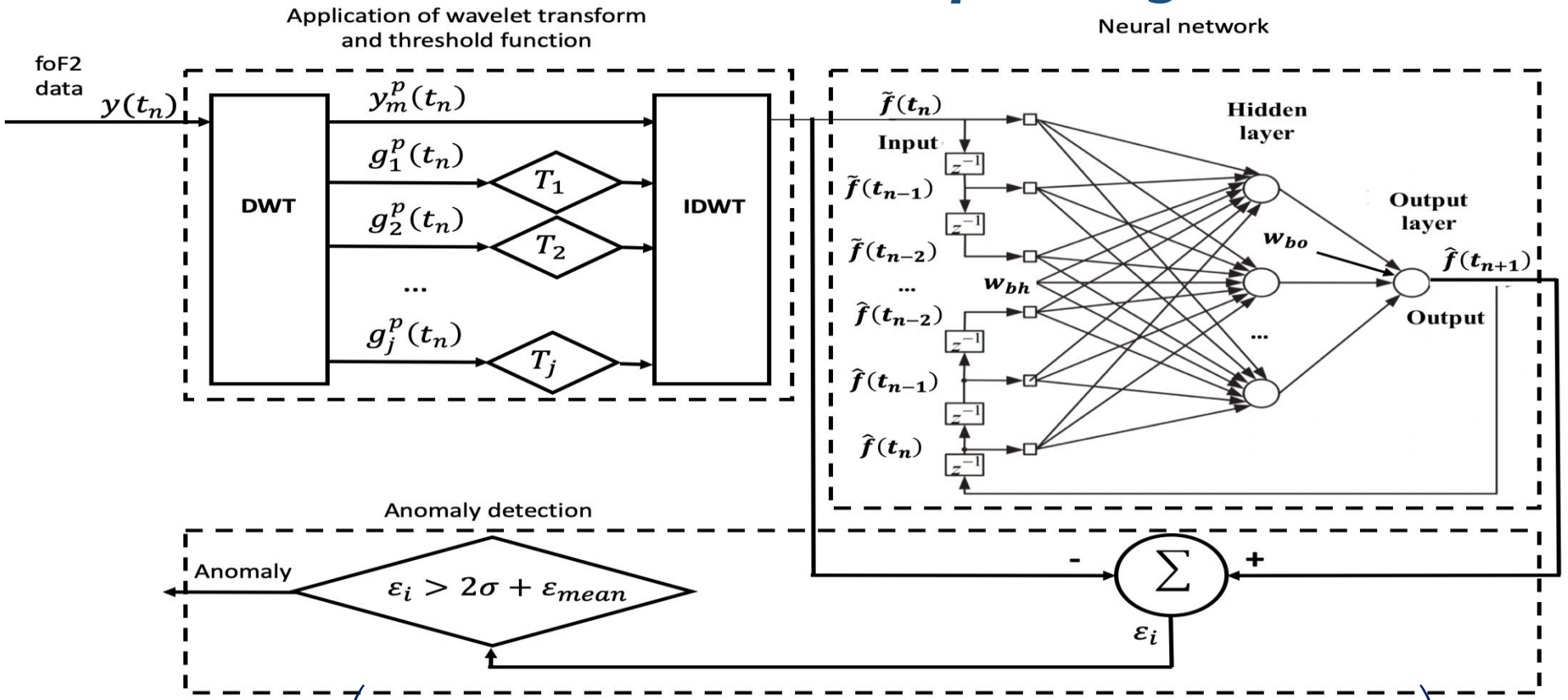

$$\hat{f}(t_{n+1}) = F_o\left(w_{bo} + \sum_{h=1}^{D} w_{ho} \cdot F_h\left(w_{bh} + \sum_{i=0}^{l_{\tilde{f}}} w_{ih}\tilde{f}(t_{n-i}) + \sum_{z=0}^{l_{\hat{f}}} w_{zh}\hat{f}(t_{n-z})\right)\right)$$

$$\tilde{f}(t_n) = y_m^p(t_n) + \sum_{j,k} P_{T_j^p}(d^p{}_{j,k})\Psi_{j,k}^p(t_n), \qquad P_{T_j^p}(d^p{}_{j,k}) = \begin{cases} d^p{}_{j,k}, \text{если } |d^p{}_{j,k}| \geq T_j^p, \\ 0, \text{если } |d^p{}_{j,k}| < T_j^p. \end{cases}$$

An algorithm for anomaly detection in foF2 data using NARX and threshold wavelet filtering

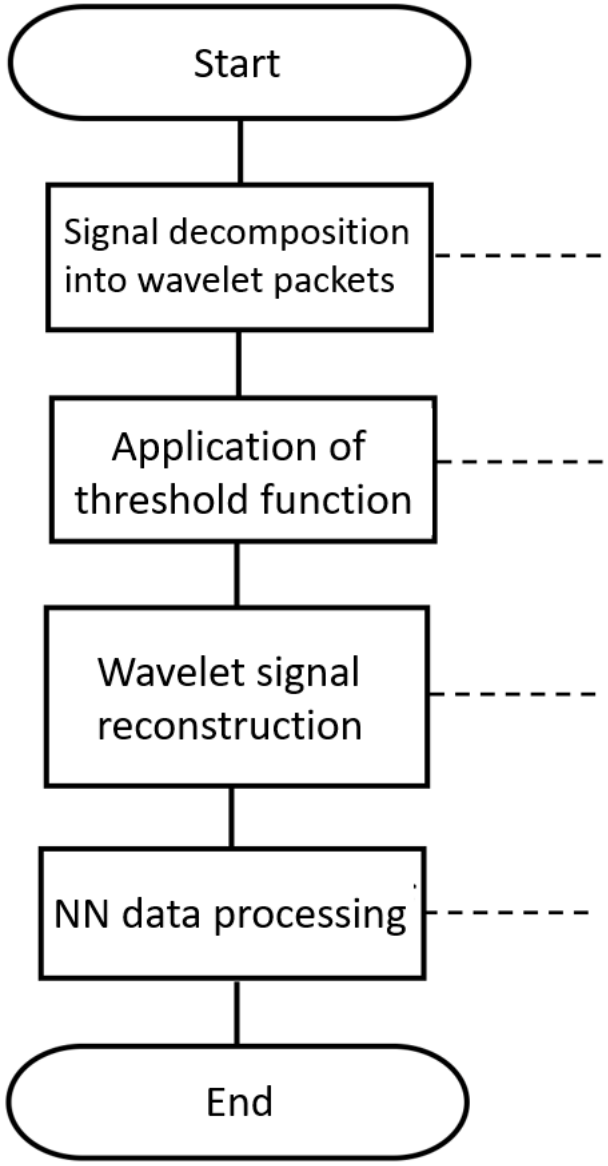

$$y(t_n) = y_m^p(t_n) + \sum_j g_j^p(t_n),$$

$$y_m^p(t_n) = \sum\nolimits_k {c^p}_{m,k}\phi_{m,k}^p(t_n)$$

$$g_j^p(t_n) = \sum\nolimits_k {d^p}_{j,k}\Psi_{j,k}^p(t_n).$$

$$T_j({d^p}_{j,k}) = \begin{cases} {d^p}_{j,k}, \text{if } |{d^p}_{j,k}| \geq T_j, \\ 0, \text{if } |{d^p}_{j,k}| < T_j. \end{cases}$$

$$\tilde{f}(t_n) = y_m^p(t_n) + \textstyle\sum_{j,k} T_j({d^p}_{j,k})\Psi_{j,k}^p$$

$$\hat{f}(t_{n+1}) = F_o\left(w_{bo} + \textstyle\sum_{h=1}^{D} w_{ho} \cdot \right.$$

$$\left. F_h\left(w_{bh} + \textstyle\sum_{i=0}^{l_{\tilde{f}}} w_{ih}\,\tilde{f}(t_{n-i}) + \right.\right.$$

Processing of data during a moderate storm on July 17, 2017

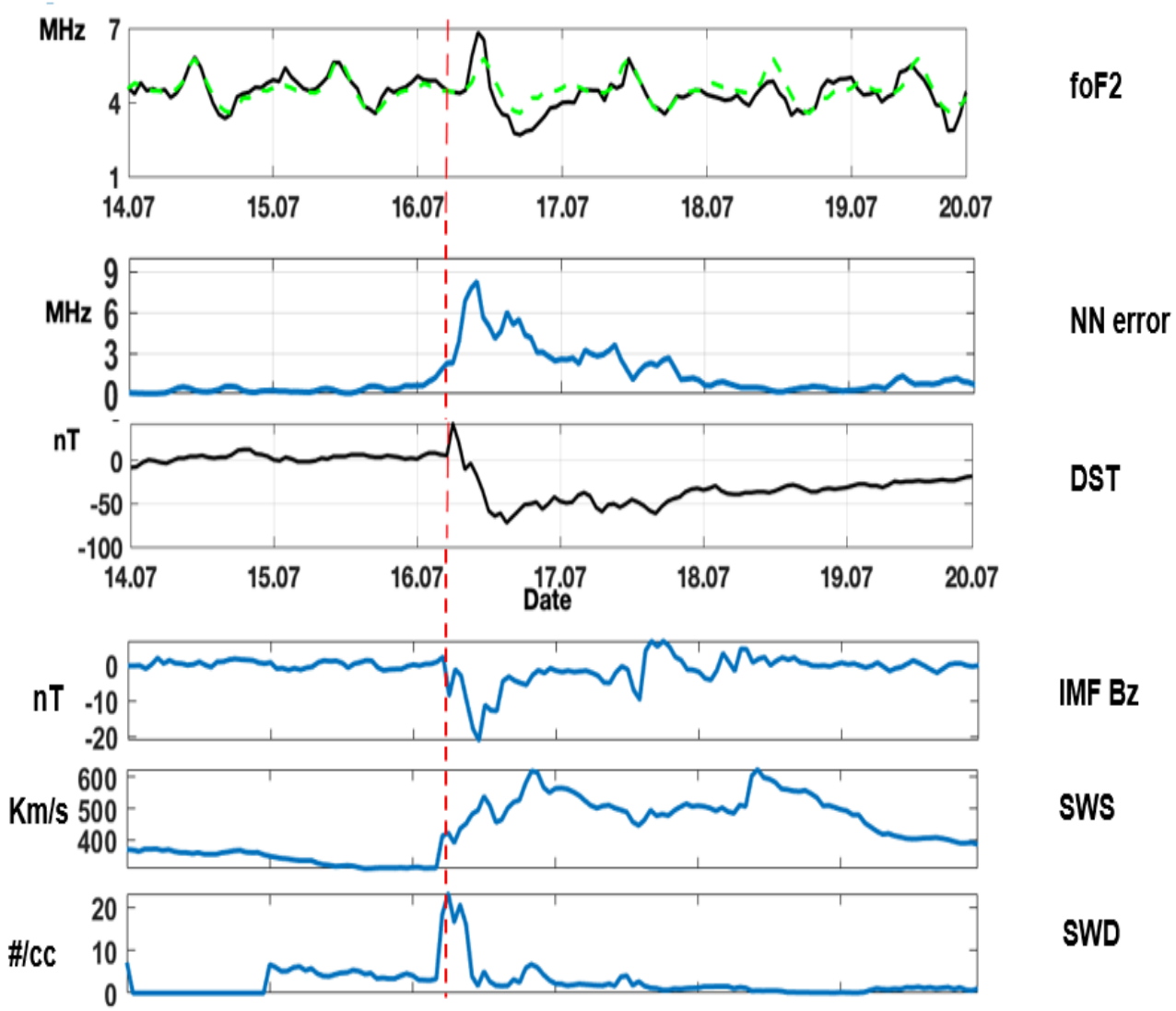

Moderate magnetic storm with gradual commencement on February 10, 2022

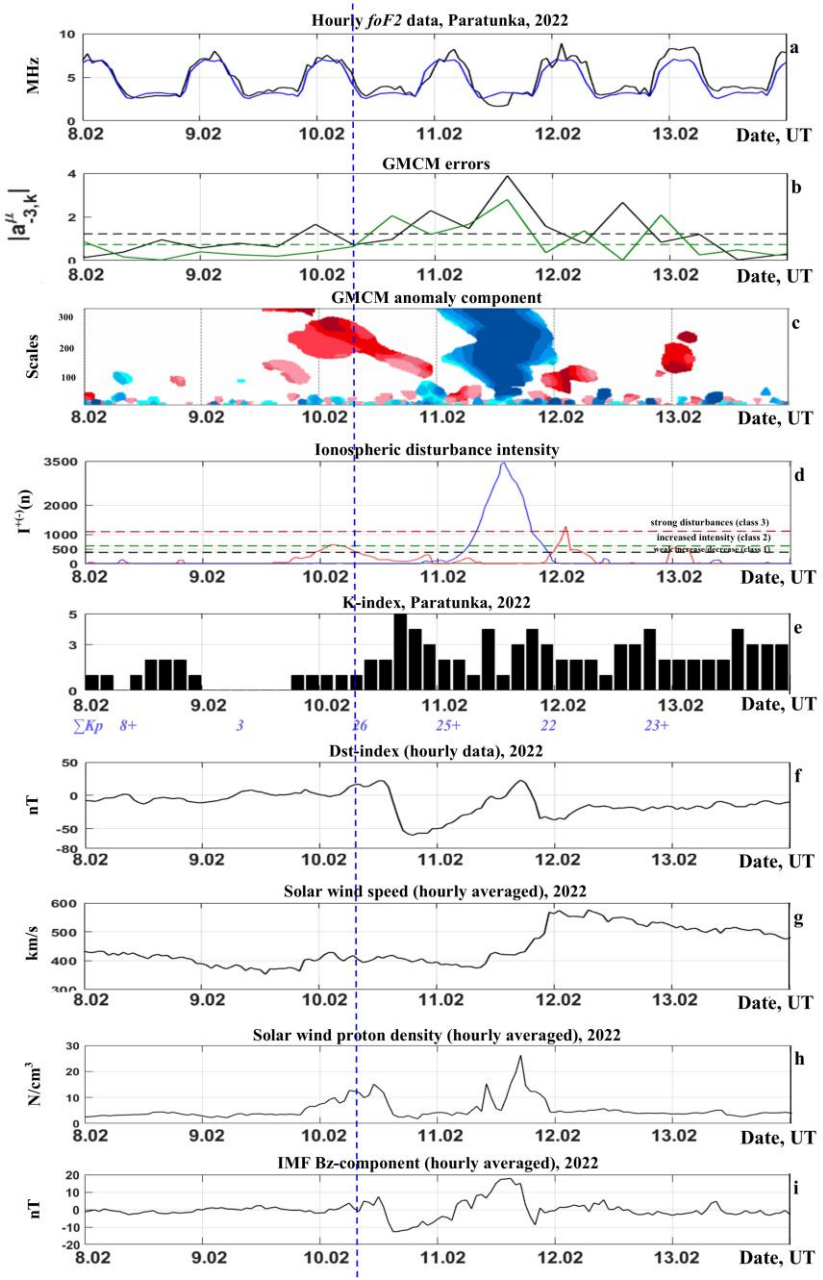

During the CME arrival (http://ipg.geospace.ru), there was a smooth increase in foF2 exceeding the anomalous threshold 6 hours before the event. During the formation of the anomaly, a strong correlation with solar wind parameters is observed.

During the recovery phase, a high-intensity negative ionospheric anomaly occurred. At the beginning and in the second half of the day on February 11, an inhomogeneous accelerated flux arrived from two CMEs and CIR. IMF southern component fluctuations intensified to Bz = - 16 nT, solar wind speed reached 600 km/s. A significantly increase of disturbances in near-Earth space was accompanied by intense decrease in foF2. At the end of the day on February 11, a short-term positive ionospheric anomaly occurred at the background of a sharp increase in SWS and a southward turn of IMF component.

Moderate magnetic storm with gradual commencement on April 16, 2021

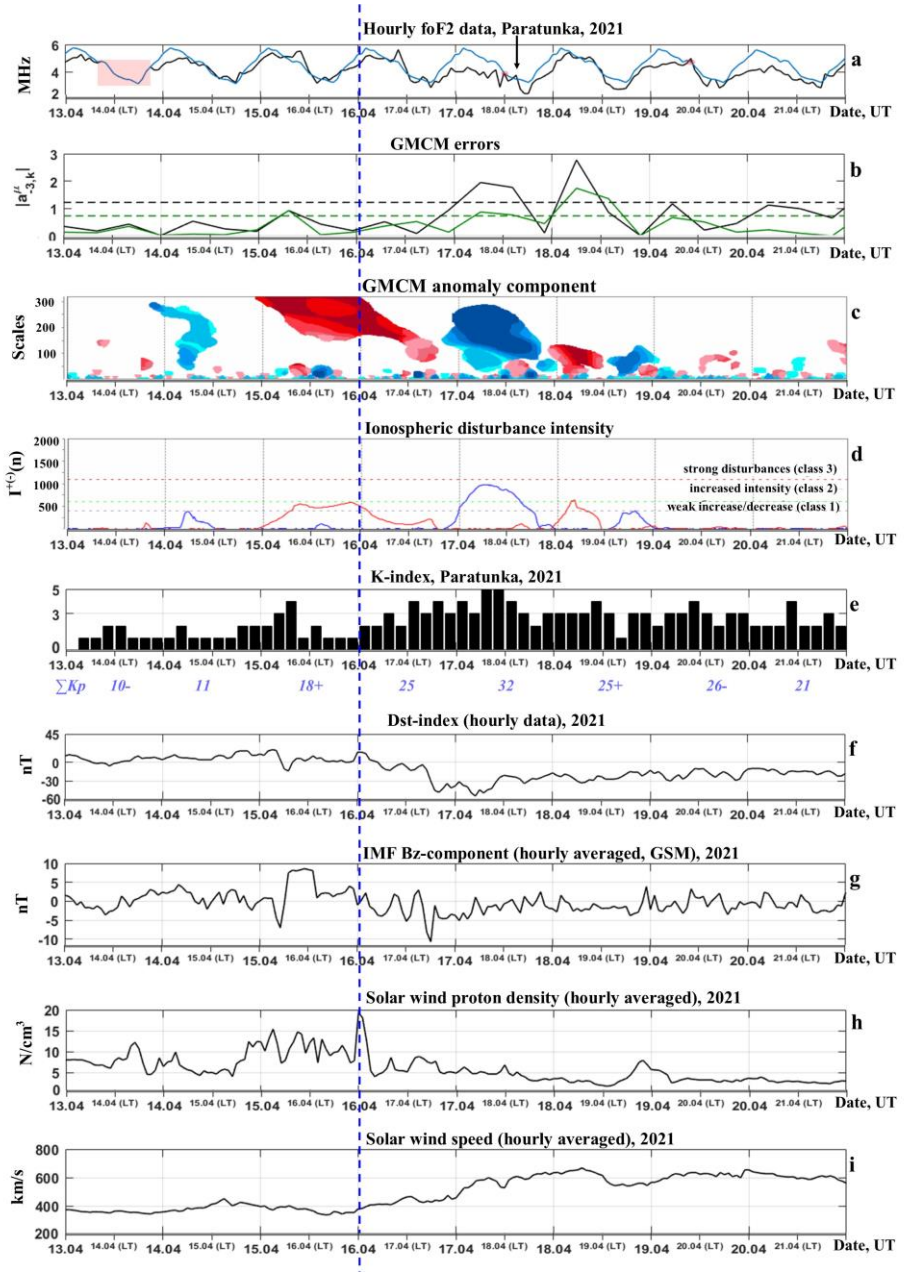

On the eve of the event, background oscillatory processes occurred in the ionosphere. At the beginning of the day on April 15, a smooth anomalous increase in foF2 of weak intensity is observed at the background of a weakly disturbed geomagnetic field. The positive anomaly formed 18 hours before the magnetic storm with gradual commencement. The anomaly may be associated with an inhomogeneous accelerated flow from CME, which arrived at the end of the day on April 14 (http://ipg.geospace.ru). The period of anomaly formation coincides with the period of sharp southward rotation and intensification of fluctuations of IMF Bz-component, increase of solar wind density and insignificant increase of geomagnetic activity.

During the recovery phase, a negative anomaly of moderate intensity was formed. Recovery of the level of foF2 fluctuations is observed since April 18 (positive anomaly of class 1). During the storm, an earthquake with a magnitude of 5.9 occurred in Kamchatka (https://sdis.emsd.ru/), the moment of the earthquake is marked with a vertical arrow.

Strong magnetic storm with gradual commencement on May 27, 2017

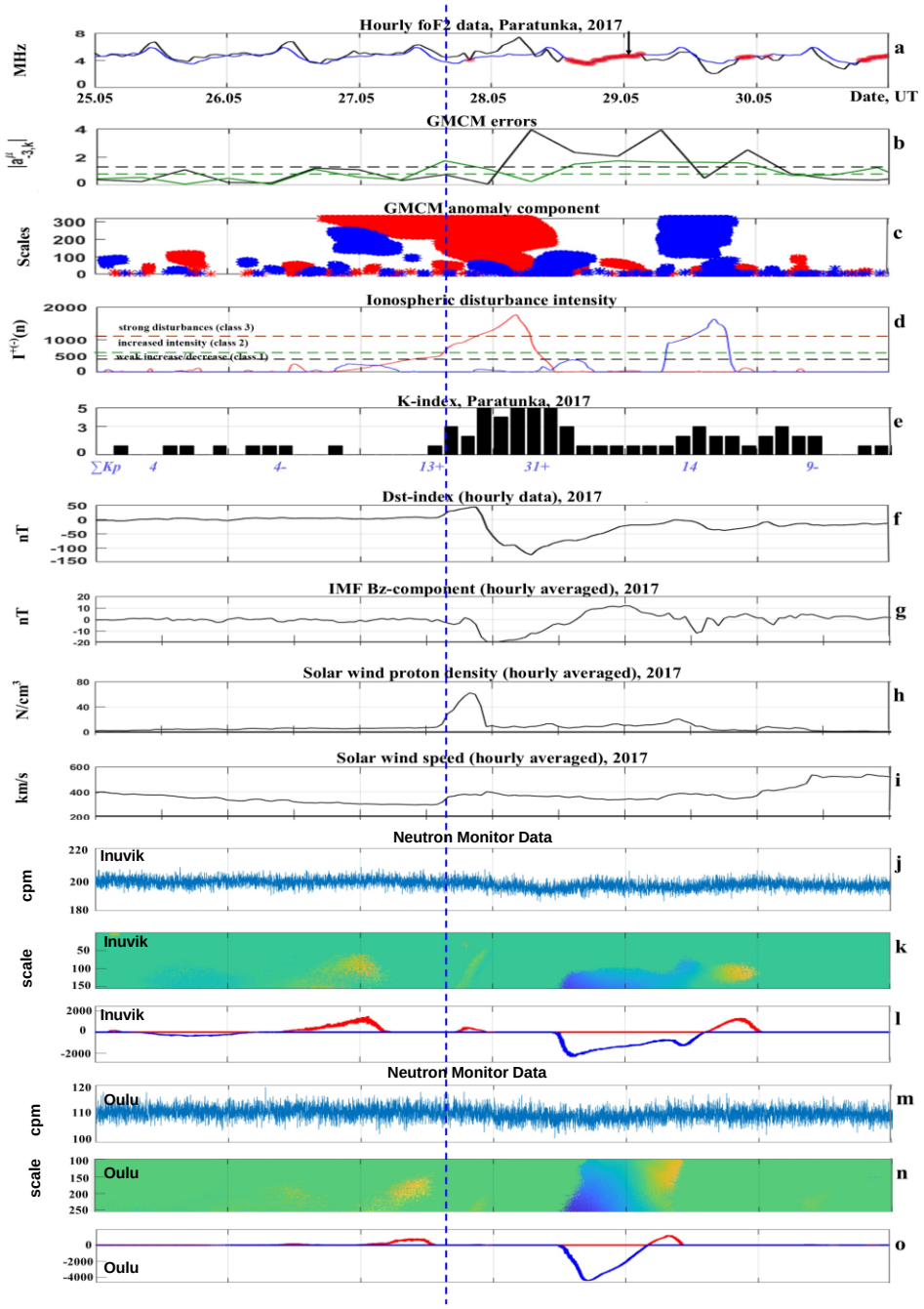

At the background of quiet geomagnetic field and NES parameters, a smooth increase in foF2 is observed, which exceeded the anomalous threshold 3 hours before the event. The positive anomaly reached its maximum intensity during the storm's main phase. During this period, a sharp expansion of the spectrum into the high-frequency range is observed correlating with a significant increase in solar wind density and a southward turn and intensification of IMF component fluctuations.

During the event, there were long gaps in the foF2 data (marked in red), which were filled with the 27-day median values for processing. During the recovery phase of the storm, a negative anomaly of high intensity occurred.

Strong magnetic storm with gradual commencement on February 26-27, 2023

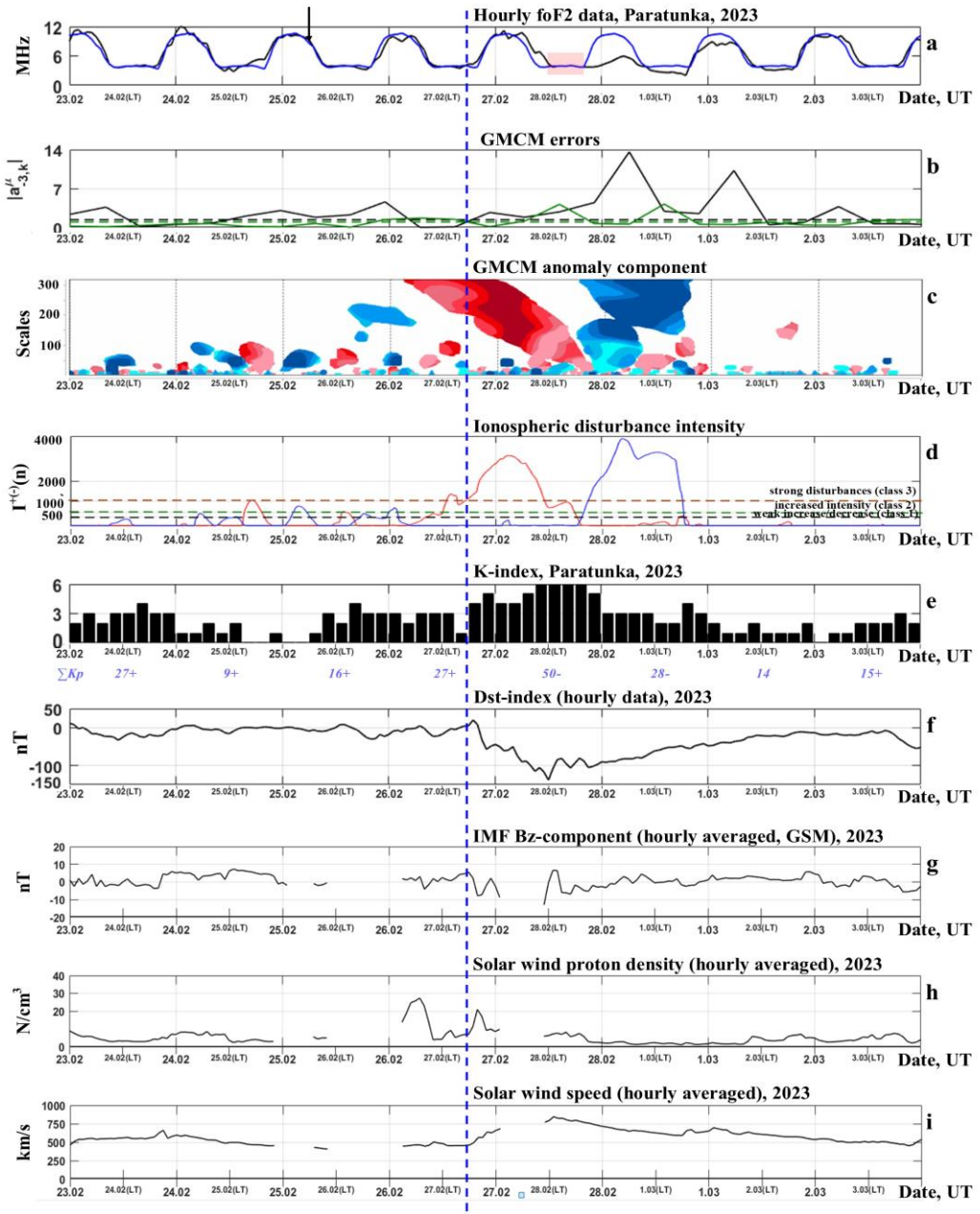

On the eve of the storm, anomalous oscillatory processes of moderate intensity are observed in the ionosphere, which are probably related to the earthquake with magnitude 5.4 that occurred in Kamchatka on February 25 (https://sdis.emsd.ru/). The moment of the earthquake is marked on the vertical arrow. In the first half of the day on February 25, there was an inhomogeneous accelerated flux from CME and CIR (http://ipg.geospace.ru). During this period, geomagnetic activity increased slightly. At 07.// UTC on February 26, an inhomogeneous accelerated flux from two CMEs arrived, solar wind speed by the end of the day was 770 km/s. During the period of CME arrival, at the background of a sharp increase of solar wind density, an anomalous increase in foF2 occurred, which 4 h before the onset of the magnetic storm led to the formation of a positive anomaly of high intensity.

During the main phase of the storm, the positive anomaly reached very high values (more than 3000 conventional units). During the recovery phase, a negative anomaly of very high intensity was formed (about 4000 conventional units).

Moderate magnetic storm with gradual commencement on April 20, 2018

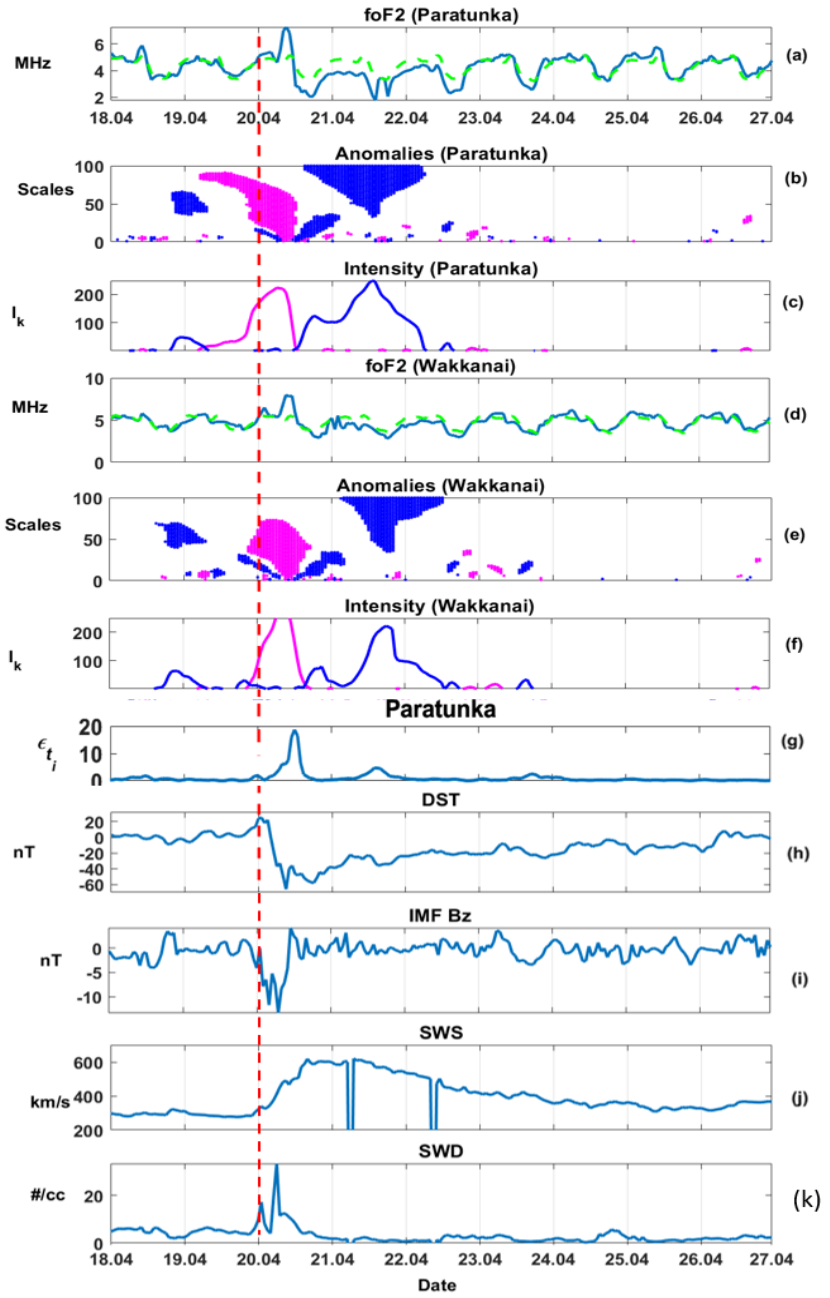

At the end of day on April 19, an accelerated flux arrived from CIR (http://ipg.geospace.ru). During the period of CIR arrival, there was a sharp anomalous increase of electron concentration of the ionosphere at the stations. The exceedance of anomalous threshold was recorded at Paratunka station 3-4 h earlier than at Wakkanai station. *The disturbance of geomagnetic field on April 20 was observed at all latitudes*. Formation of a positive ionospheric anomaly of high intensity is observed in the first hours of April 20. It occurred at the background of intense increase of density and speed of solar wind and a sharp southward rotation of IMF component. The observed general anomalous dynamics of ionospheric process at the stations indicates a large scale of disturbance. The positive ionospheric anomaly reached its maximum intensity during the main phase of the magnetic storm. At the recovery phase, a negative ionospheric anomaly of high intensity was formed. The foF2 variations was recovered for more than 2 days.

Strong magnetic storm with gradual commencement on August 25, 2018

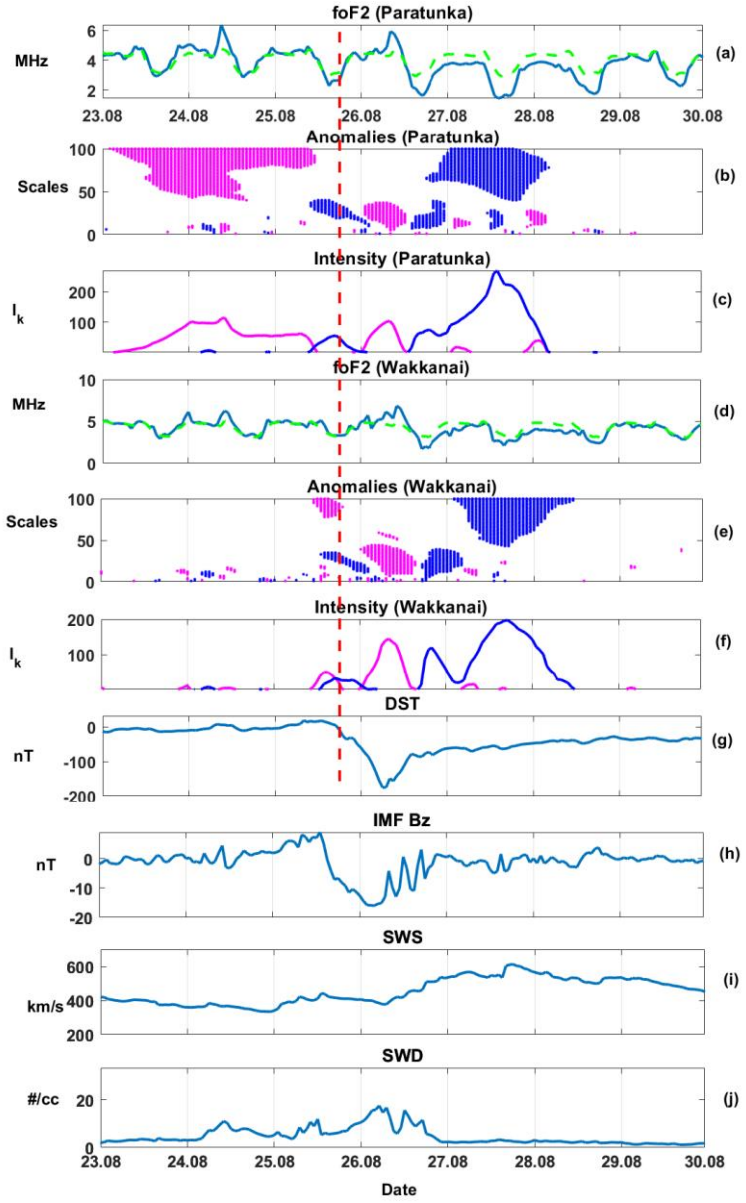

Due to CME, geomagnetic disturbance was registered on August 25 at some hours of the day at the middle latitudes and by some high-latitudinal stations (http://ipg.geospace.ru). On the eve of the storm, there was a smooth anomalous increase of electron concentration at Paratunka station. The anomaly reached the highest intensity on August 24 at the period of increased fluctuations of IMF southern component and local increase of solar wind density. At the time of the peak of the positive anomaly intensity, a magnetic storm occurred at high latitudes (August 24 at 12.// UT at Barentsburg station). At the middle latitudes, the geomagnetic field at this period was very quiet. One should note that the anomaly in the ionosphere is observed at Paratunka station (53.0°N and 158.7°W) and absent at Wakkanai station (45.16°N and 141.75°W).

During the storm at the stations, the general anomalous dynamics of ionospheric process was clearly pronounced. At the initial phase, electron concentration was anomalously decreased. At the beginning of the day on August 26, an accelerated flux from CIR arrived. Solar wind speed reached over 650 km/s on August 27, the fluctuations of IMF southern component increased to Bz=±17 nT. During this period, there was a sharp increase of electron concentration - a positive ionospheric anomaly of moderate intensity. At the recovery phase, a long-term (about 2 days) negative ionospheric anomaly was formed at the stations.

Moderate magnetic storm with gradual commencement on July 16, 2017

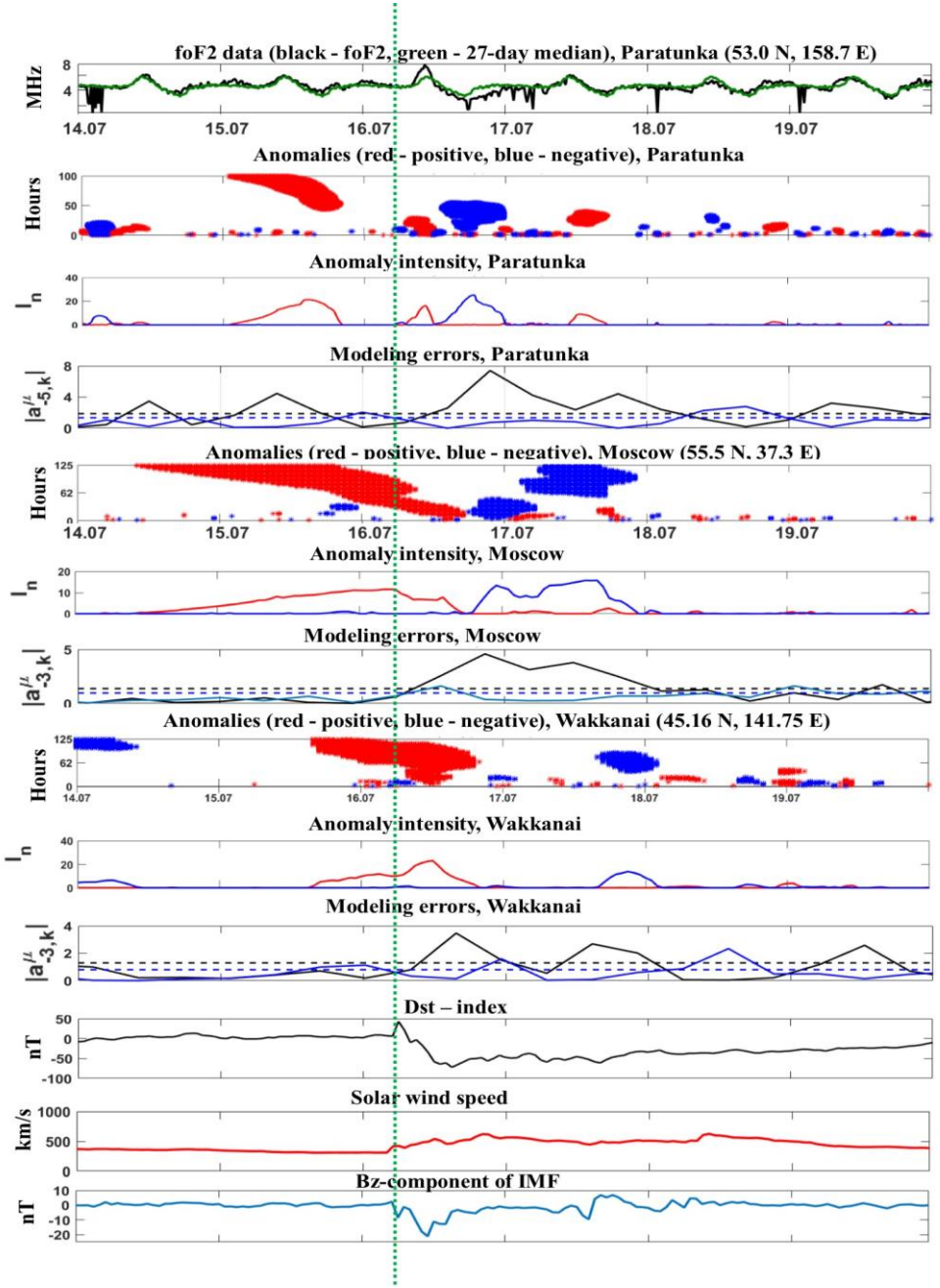

Positive anomalies in foF2 precede the commencement of the magnetic storm. These anomalies were occurred 35 hours before the storm commencement at the Paratunka and Moscow stations, and 15 hours before at the Wakkanai station. Application of the median method in comparison with GMCM did not allow to detect this anomalous change in ionospheric parameters.

During the storm's initial phase, electron concentration in the ionosphere remained anomalously increased. This is may be due to the penetration of the electric field into the middle and low latitudes.

Anomalous decrease in electron concentration observed during the recovery phase at the *Paratunka* and *Moscow* stations occurred with a difference of several hours and lasted about 26 hours (at the Paratunka station, there were gaps in the data from 10:15 to 23:45 on July 17, 2017). The negative anomaly is likely to be associated with heating and elevation of the thermosphere, which lead to the recombination rate increase and, as a sequence, to the ionization depletion.

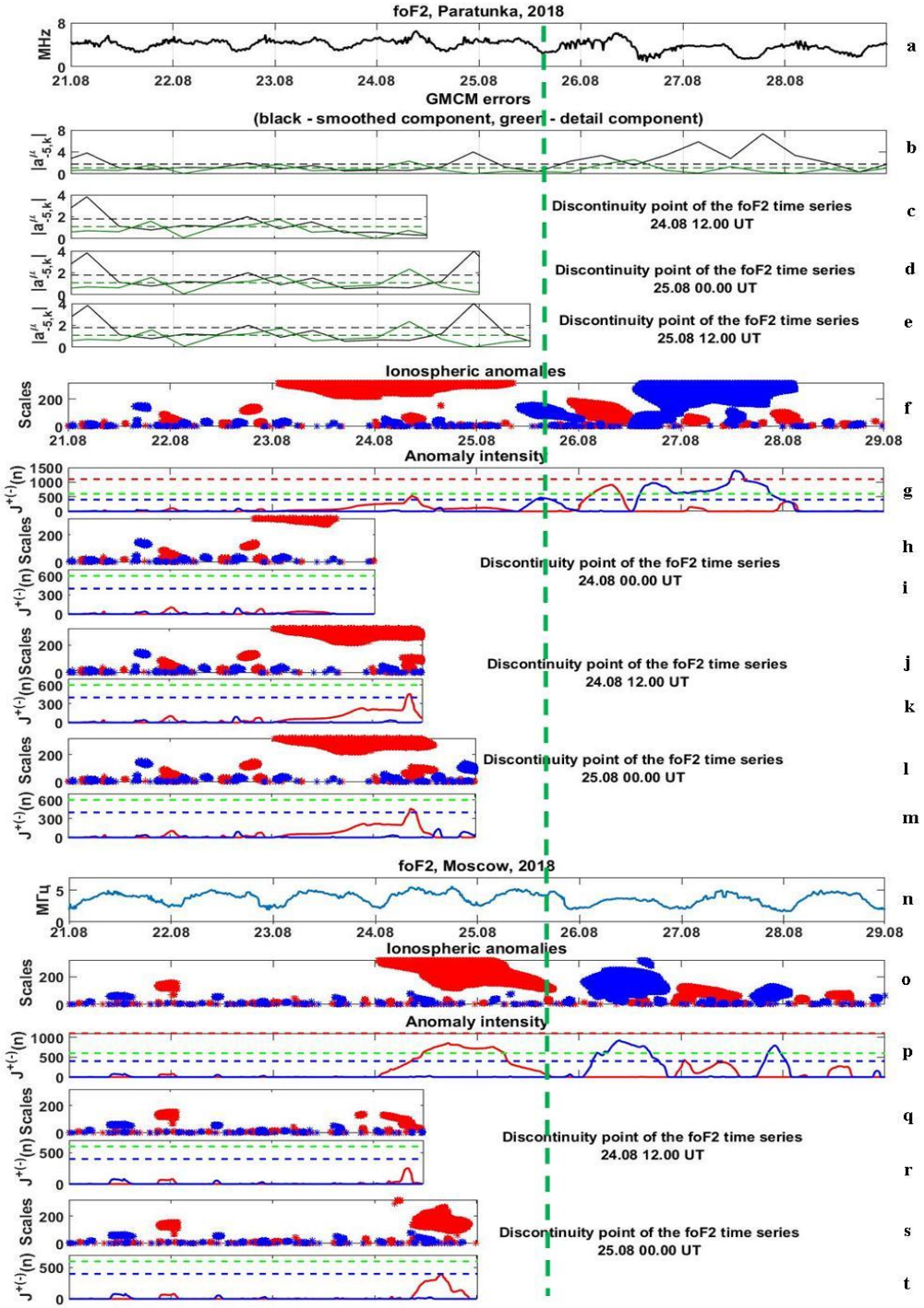

Anomaly detection in operational mode (Paratunka and Moscow stations)

There is anomalous increase of weak intensity in foF2 on the eve of a strong magnetic storm on August 25, 2018. During the storm, oscillatory processes are observed in the ionosphere.

The results confirm the efficiency of the method for timely detection of sudden ionospheric anomalies of weak intensity. The positive anomaly exceeded the threshold on August 24 at 09.00 UT at Paratunka station and approached the threshold level 7 hours later at Moscow station .

During the event, a typical dynamics of the ionosphere parameters during the disturbed period was observed (according to the Paratunka station data): during the initial phase, electron concentration of the ionosphere remained increased, at the recovery phase the electron concentration significantly decreased and intense negative ionospheric storms occurred.

Anomaly detection in foF2 data in operational mode, 2016.

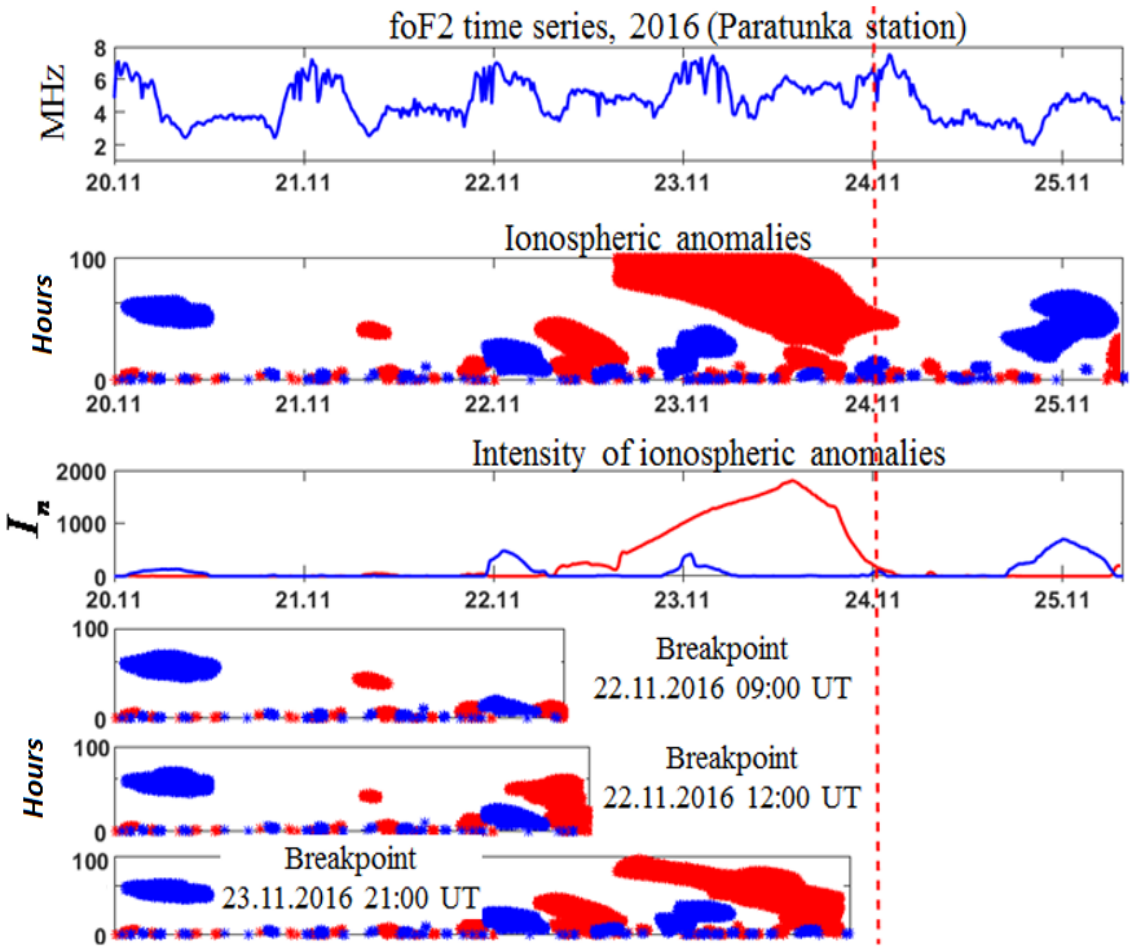

Aurora interactive program system of complex data analysis **:**
http://lsaoperanalysis.ikir.ru:9180/lsaoperanalysis.html

Analysis of foF2 data under quiet conditions

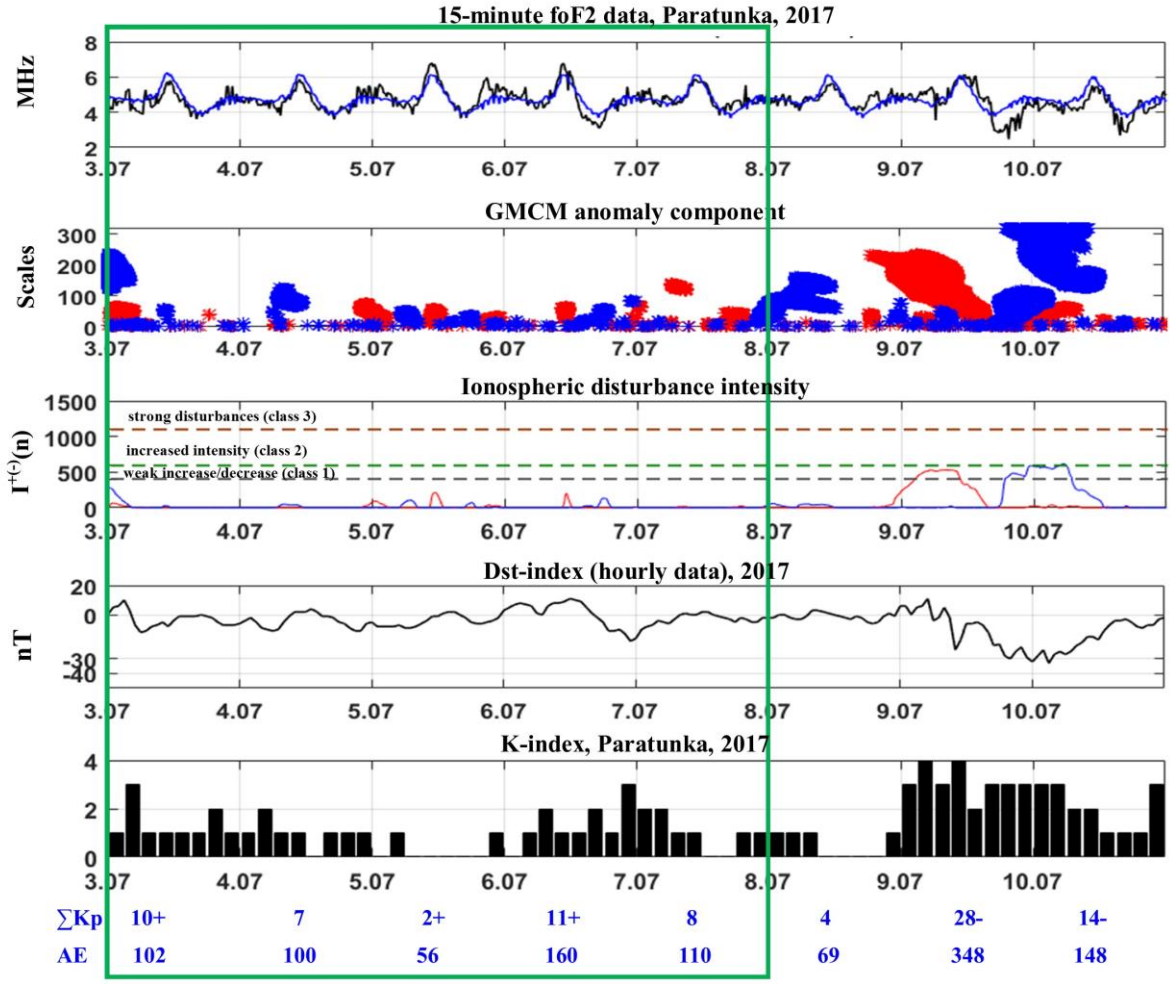

season	number of quiet days	number of days with sudden anomalies that reached the threshold	max/average intensity of oscillatory processes in the ionosphere
winter	54	5	325 (max) / 119 (average)
summer	40	-	250 (max) / 106 (average)

Results analysis

The considered events show the general character of the ionospheric process dynamics during magnetic storms - a smooth increase in foF2 before the onset of the events, and reaching the maximum intensity of anomaly during the initial or main phase of the storm. During the recovery phase, the foF2 time variations change significantly and there is an anomalous decrease of electron concentration.

A detailed analysis of pre-storm ionospheric anomalies and comparison with near-Earth space parameters and magnetosphere indicate their possible connection with solar processes. The increase of electron concentration exceeds the anomalous threshold several hours before the development of magnetic storms. The formation of anomalies is observed at a quiet or weakly perturbed geomagnetic field, correlates with southward rotations and an increase of IMF Bz-component fluctuations and increases of solar wind density. In most cases, the pre-increase effect in foF2 was observed for magnetic storms originated due to the arrival of CME. Results confirm high frequency of the pre-increase effect in the ionosphere and agree with the results of the papers [Danilov et al. (2019, 2020, 2022), Joshua et al. (2021)]. But, undoubtedly, clarification of the nature of pre-storm anomalies requires further comprehensive studies involving more statistics, as well as expanding the set of NES parameters and data mining methods.

The positive anomalies observed during storm may be due to the penetration of the electric field into middle and low latitudes (PPEF effect). Negative phase formation mechanisms are likely influenced by thermosphere heating and elevation, resulting in an increase in the recombination rate and a subsequent decrease in ionization within the F-layer of the ionosphere. The time course for foF2 recovery lasts at least two days. Note that during strong geomagnetic disturbances, the intensity of ionospheric anomalies can reach very high values and exceed significantly the threshold of class 3.

Method for analyzing neutron monitor data and detecting anomalies in cosmic ray variations

Bogdana Mandrikova

$$f(t) = \begin{bmatrix} R(t) + e_R(t) \\ A(t) + e_A(t) \end{bmatrix} = \begin{bmatrix} \sum_R S_R(t) + e_R(t) \\ \sum_M S_M(t) + e_A(t) \end{bmatrix} = \begin{bmatrix} L\left(\theta^{(q)}\left(\dots\left(h_1\left(\theta^{(1)} f\right)\right)\right)\right) + e_R(t) \\ \sum_M \sum_k \alpha_k \langle f, \Psi_{M,k}\rangle \Psi_{M,k}, + e_A(t) \end{bmatrix}$$

NM data

f_Z

Construction of a nonlinear circuit

wavelet packets

$f_m^p(t)$, $g_1^p(t)$, $g_2^p(t)$, $\vdots$, $g_m^p(t)$

$$B_{j_i}^{p_i} = \begin{cases} \{\Psi_{j_i}^{p_i}(2^{j_i}t - m)\}_{m\in\mathbb{N}}, \text{если } \sum_{m\in I^{p_i}} \left|\left\langle f_Z, \Psi_{j_i,m}^{p_i}\right\rangle\right|^2 \geq \sum_{m\in I^{2p_i}} \left|\left\langle f_Z, \Psi_{j_i+1,m}^{2p_i}\right\rangle\right|^2 + \sum_{m\in I^{2p_i+1}} \left|\left\langle f_Z, \Psi_{j_i+1,m}^{2p_i+1}\right\rangle\right|^2 \\ \left\{\Psi_{j_i+1}^{2p_i}\right\}_{m\in\mathbb{N}} \cup \left\{\Psi_{j_i+1}^{2p_i+1}\right\}_{m\in\mathbb{N}}, \text{если } \sum_{m\in I^{p_i}} \left|\left\langle f_Z, \Psi_{j_i,m}^{p_i}\right\rangle\right|^2 < \sum_{m\in I^{2p_i}} \left|\left\langle f_Z, \Psi_{j_i+1,m}^{2p_i}\right\rangle\right|^2 + \sum_{m\in I^{2p_i+1}} \left|\left\langle f_Z, \Psi_{j_i+1,m}^{2p_i+1}\right\rangle\right|^2 \end{cases}$$

$T_{j_i}^h = t_{1-\frac{\alpha}{2},h-1}\,\hat{\sigma}_{j_i}^h$, $t_{\alpha,N}$ – α- quantiles of the Student's t distribution, $\hat{\sigma}_j$ – RMS

$$\varepsilon_Z^2 = \sum_{j_i}\sum_m T_{j_i}^p \left(\langle f_Z, \Psi_{j_i,m}^{p_i}\rangle\right) \Psi_{j_i,m}^{p_i} .$$

Autoencoder

$$f'_Z = h^{(l)}\left(V^{(l)}\left(\dots\left(h^{(1)}\left(V^{(1)} f_Z + b^{(1)}\right)\right)\right) + b^{(q)}\right)$$

$$\varepsilon_Z^1 = f_Z\text{-}f'_Z$$

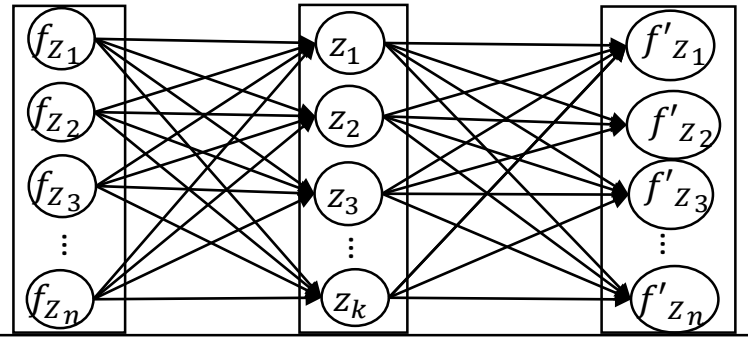

ε_Z^2

ε_Z^1

Application of adaptive thresholds and anomaly intensity assessment

$$P_{T_j^q}\left[W\varepsilon_Z\left(\frac{1}{2^j},\frac{k}{2^j}\right)\right] = \begin{cases} W\varepsilon_Z\left(\frac{1}{2^j},\frac{k}{2^j}\right), \left|W\varepsilon_Z\left(\frac{1}{2^j},\frac{k}{2^j}\right)\right| \geq T_j^q, \\ 0, \left|W\varepsilon_Z\left(\frac{1}{2^j},\frac{k}{2^j}\right)\right| < T_j^q. \end{cases}$$

$T_j^q = t_{1-\frac{\alpha}{2},q-1}\,\hat{\sigma}_j^q$, $t_{\alpha,N}$ – α- quantiles of the Student's t distribution, $\hat{\sigma}_j^q$ – RMS,

$$\hat{\varepsilon}_Z = \sum_{j=0}^{J}\sum_{k=1}^{K} P_{T_j^q}\left[W\varepsilon_Z\left(\frac{1}{2^j},\frac{k}{2^j}\right)\right]\Psi_{jk}$$

$$E_{t_i} = \left|\sum_{j=0}^{J} P_{T_j^q}\left[W\hat{\varepsilon}_Z\left(\frac{1}{2^j},\frac{t_i}{2^j}\right)\right]\right| > 0$$

E_t^1

E_t^2

Decisive rule (classification)

Anomaly detection in NM data based on neural network and adaptive thresholds

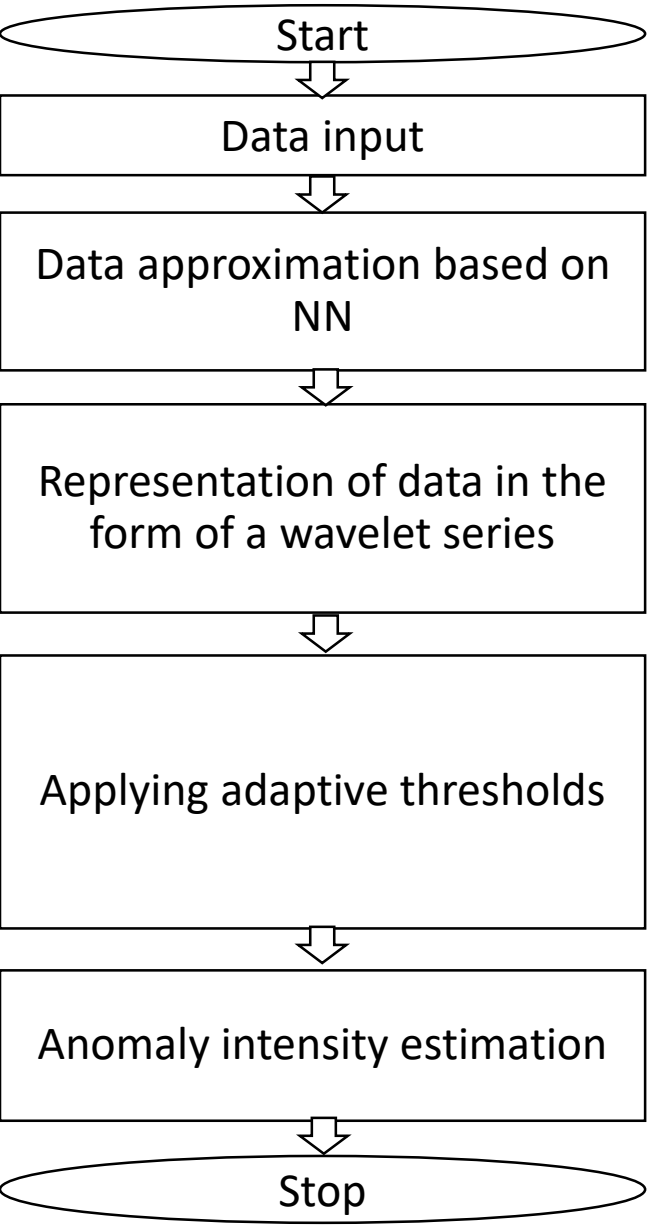

$$\{F$$

$$\{\hat{F} = h^{(2)}(\omega^{(2)}(h^{(1)}(\omega^{(1)}F + b^{(1)}) + b^{(2)})$$

$$\{\hat{F}[n] = \sum_{j,k=-\infty}^{\infty} W\hat{F}\left(\frac{1}{2^j}, \frac{k}{2^j}\right)\Psi_{jk}[n],$$

$$\{P_{T_j^l}(W\hat{F}) = \begin{cases} W\hat{F}, |W\hat{F}| \geq T_j^l \\ 0, |W\hat{F}| < T_j^l \end{cases}$$

$$\{E_k = \sum_j P_{T_j^l}|W\hat{F}|, T_j^l = t_{1-\frac{\alpha}{2},L-1}\,\hat{\sigma}_j^l$$

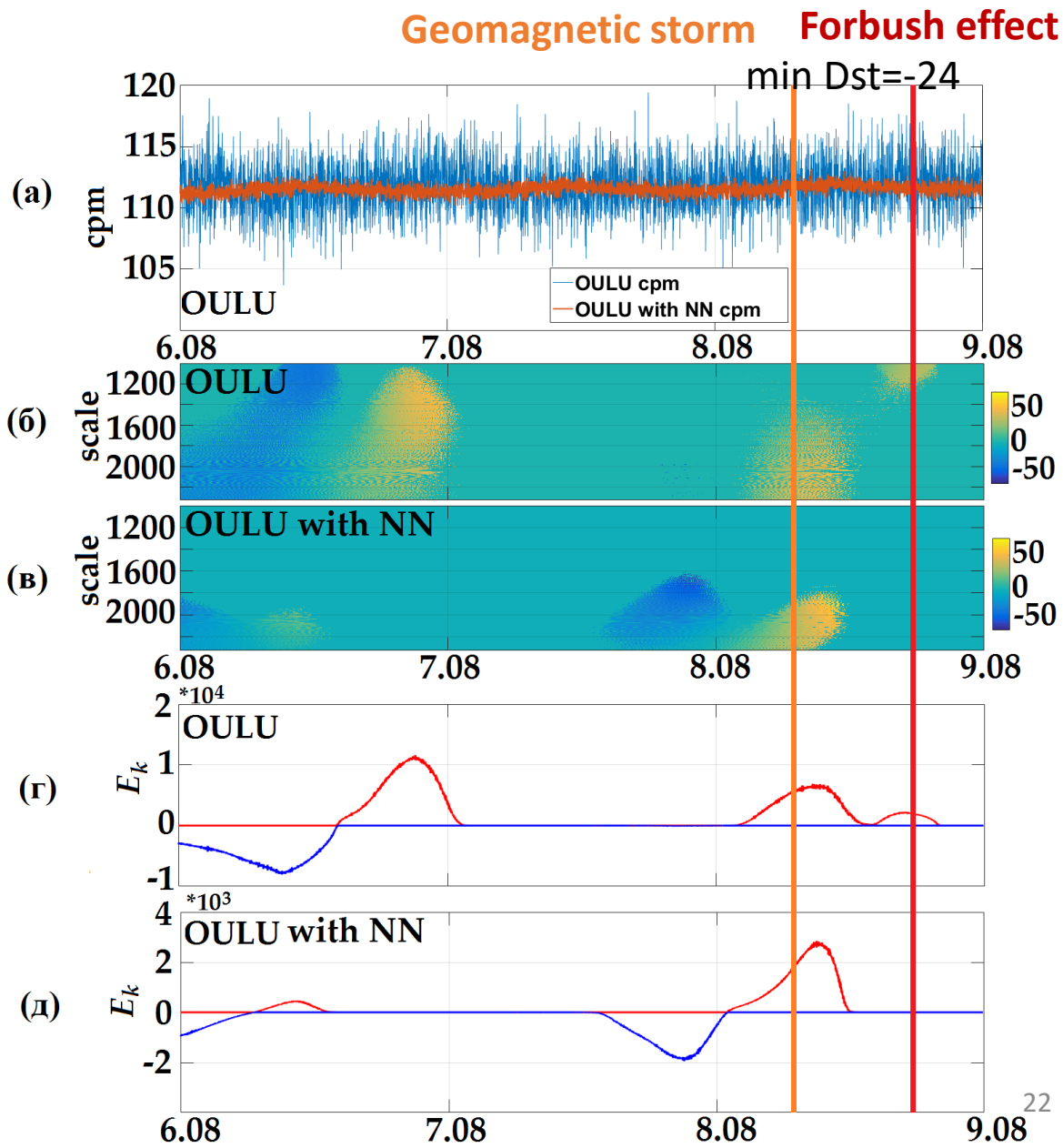

Detection of anomalies in NM data based on NAS

Start

Data input

$$F$$

Wavelet packet decomposition

$$W_j^0 = \oplus_{i=0}^{I} W_{j_i}^p, \{\Psi_{j_i}^p(2^{j_i}t - m)\}_{m\in\mathbb{N}}$$

Determining tree branches corresponding to signal components

$$B_{j_i}^p = \begin{cases} \{\Psi_{j_i}^p(2^{j_i}t - m)\}_{m\in\mathbb{N}}, \\ \sum_{m\in I^P} \frac{\left|\left\langle X, \Psi_{j_i,m}^p \right\rangle\right|^2}{\|X\|^2} \geq \sum_{m\in I^{2P}} \frac{\left|\left\langle X, \Psi_{j_i+1,m}^{2p} \right\rangle\right|^2}{\|X\|^2} + \sum_{m\in I^{2P+1}} \frac{\left|\left\langle X, \Psi_{j_i+1,m}^{2p+1} \right\rangle\right|^2}{\|X\|^2}, \\ \left\{\Psi_{j_i+1}^{2p}\right\}_{m\in\mathbb{N}} \cup \left\{\Psi_{j_i+1}^{2p+1}\right\}_{m\in\mathbb{N}}, \\ \sum_{m\in I^P} \frac{\left|\left\langle X, \Psi_{j_i,m}^p \right\rangle\right|^2}{\|X\|^2} < \sum_{m\in I^{2P}} \frac{\left|\left\langle X, \Psi_{j_i+1,m}^{2p} \right\rangle\right|^2}{\|X\|^2} + \sum_{m\in I^{2P+1}} \frac{\left|\left\langle X, \Psi_{j_i+1,m}^{2p+1} \right\rangle\right|^2}{\|X\|^2}, \end{cases}$$

Representation of data in the form of a wavelet series

$$\tilde{F}_{B_{j_i}^{p_i}}(t) = \sum_{j,k=-\infty}^{\infty} W\tilde{F}\left(\frac{1}{2^j}, \frac{k}{2^j}\right)\Psi_{jk}[n],$$

Applying adaptive thresholds

$$P_{T_j^l}(W\tilde{F}) = \begin{cases} W\tilde{F}, |W\tilde{F}| \geq T_j^l \\ 0, |W\tilde{F}| < T_j^l \end{cases}$$

Anomaly intensity estimation

$$E_k = \Sigma_j P_{T_j^l}|W\tilde{F}|, T_j^l = t_{1-\frac{\alpha}{2},L-1}\,\hat{\sigma}_j^l$$

Stop

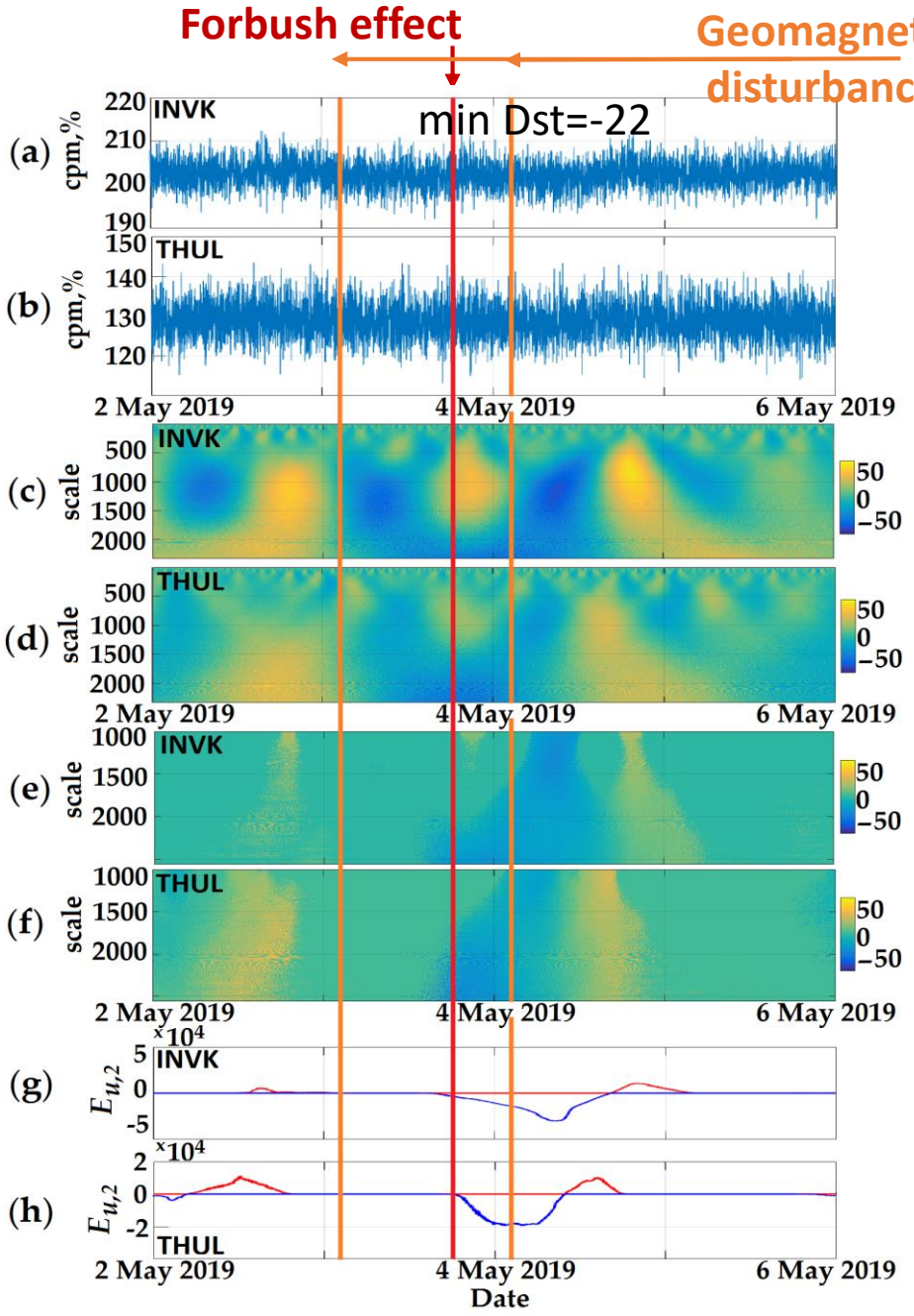

Analysis of NM data during a strong magnetic storm on November 3, 2022

On November 1, the arrivals of inhomogeneous accelerated flows from a coronal hole and a coronal mass ejection (CME) were recorded [http://ipg.geospace.ru]. The disturbances that have arisen in NES are evidenced by an increase in fluctuations of the Bz component of the IMF and a decrease in Dst. Anomalies of low intensity are observed in the NM data during this period. The results of the 2 methods are identical, which confirms their reliability.

On November 3–4, the arrival of CME was registered. A strong magnetic storm occurred at the end of the day on November 3. The results of the methods show an anomalous increase in CR intensity on the eve of the storm and a Forbush decrease of large amplitude during the period of the strongest geomagnetic disturbances on November 4.

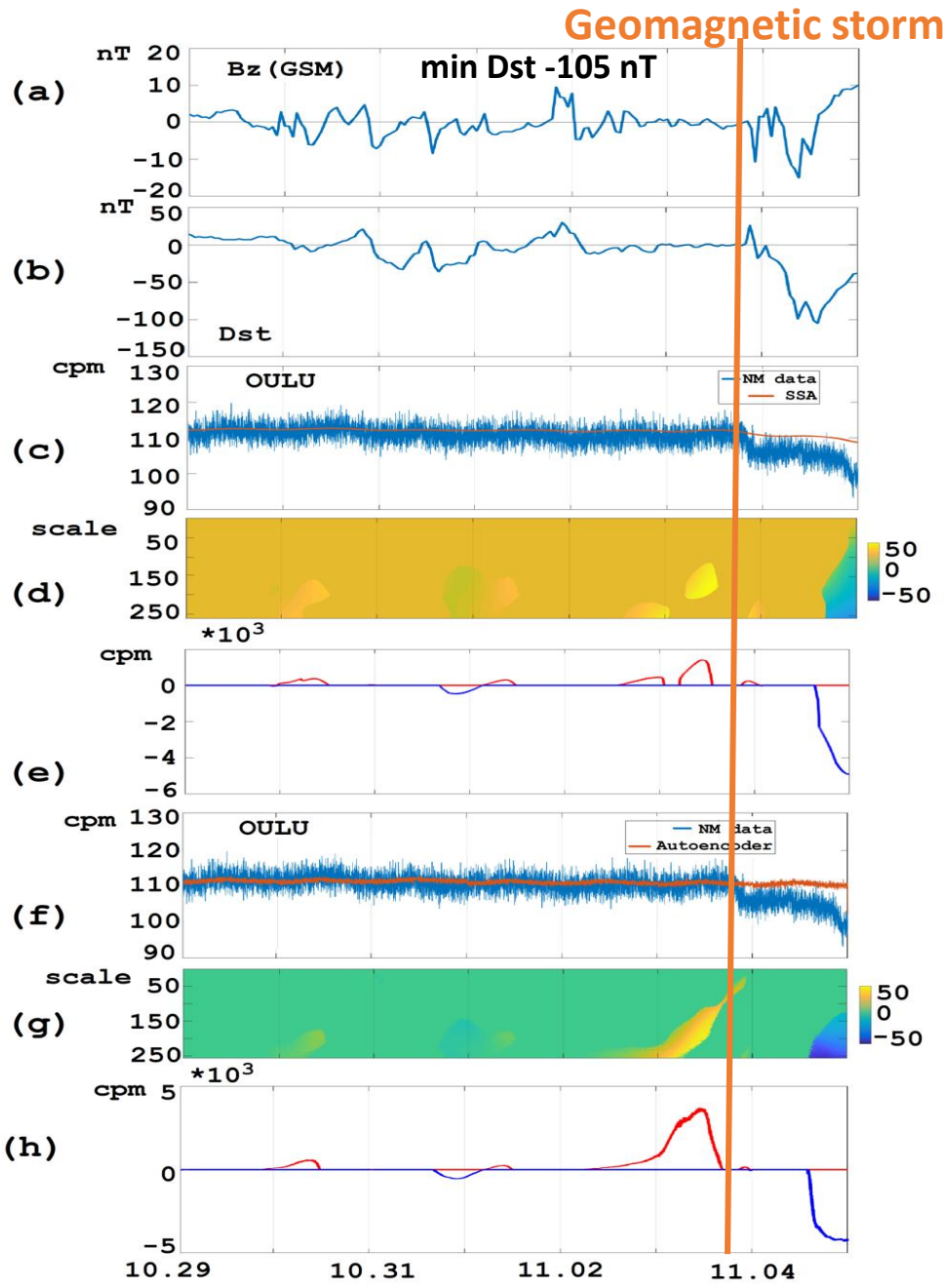

Analysis of NM data for the period March 8-28, 2022

On March 11 at 23:00 UT a weak magnetic storm arose [http://ipg.geospace.ru]. The Dst index value decreased to -51 nT, fluctuations of the Bz component of the IMF increased. According to the processing data, a sharp anomalous increase in CR intensity occurred during this period. On March 13 at 10:48 UT a moderate magnetic storm was registered (minimum Dst=-85). According to the Forbush processing data, a large amplitude decrease began at the moment of registration of the magnetic storm.

On March 27, the arrival of a heterogeneous accelerated flow from a coronal hole (CIR) and a coronal mass ejection (CME) was registered, and a geomagnetic disturbance was registered at 06:00 UT. According to the Forbush processing data, a low-amplitude decrease occurred 6 hours before the registration of the geomagnetic disturbance.

Note that the NM data component isolated on the basis of Singular Spectrum Analysis has a strong correlation with Dst.

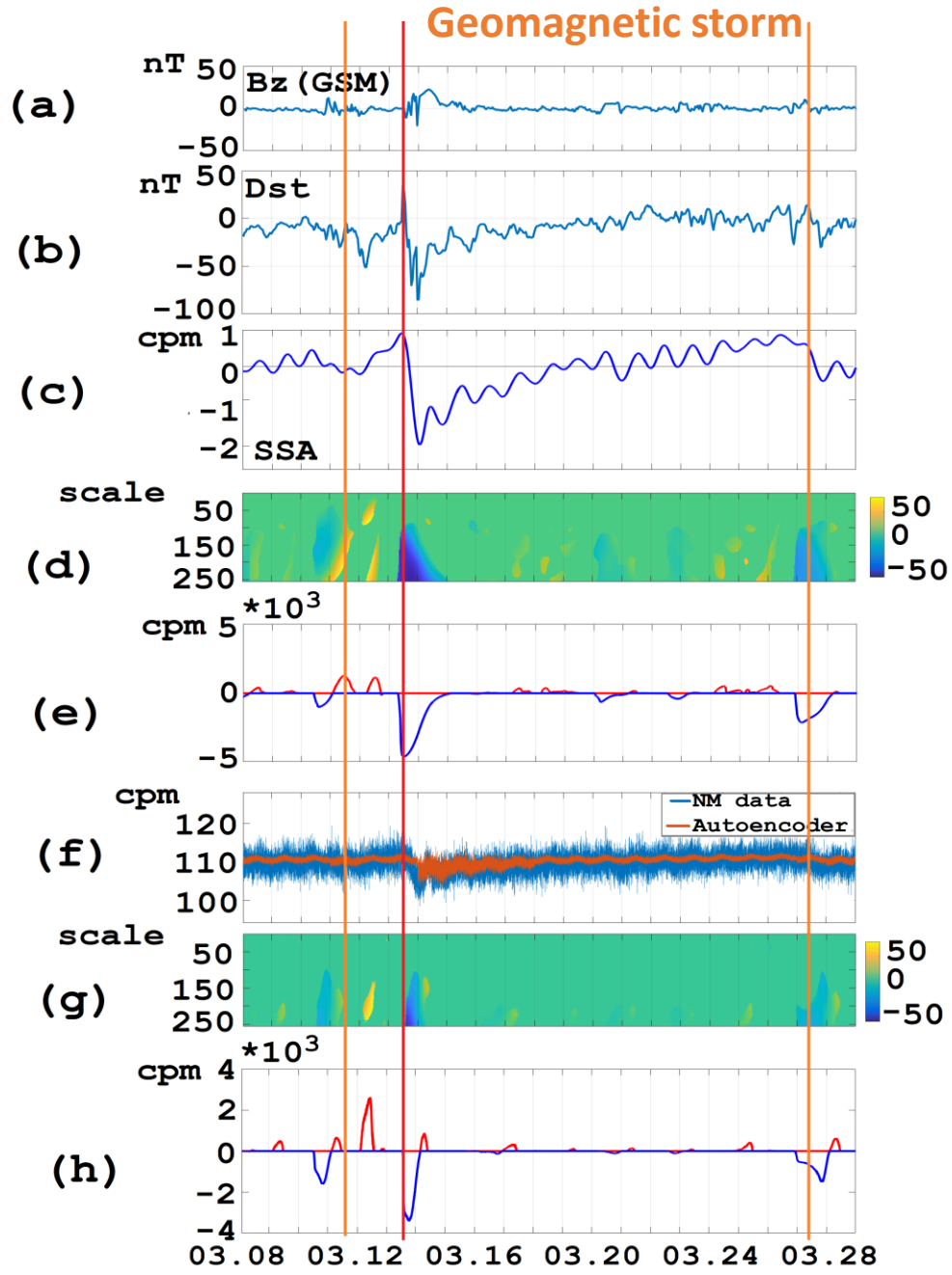

Analysis of NM data for the period August 24-30, 2021

On August 24, a heterogeneous accelerated flow from the coronal hole (CIR) arrived [http://ipg.geospace.ru]. According to the processing results, the Forbush low occurred at all analyzed stations before the first event (August 25). The detected effects in CR are apparently caused by Interplanetary Coronal Mass Ejections (ICME), which screen CR with a strong internal magnetic field and lead to Forbush effects.

On August 27, CIR and CME arrived, and a magnetic storm was recorded at 02:00 UT (min Dst = −82). Before the event at the station. An anomalous increase in CR intensity is observed in Inuvik and Thule. At the moment of a sharp turn of Bz to the south at the SOPO station, an increase in CR intensity is observed. During the main phase of the storm, short-period fluctuations in CR intensity occurred at the stations.

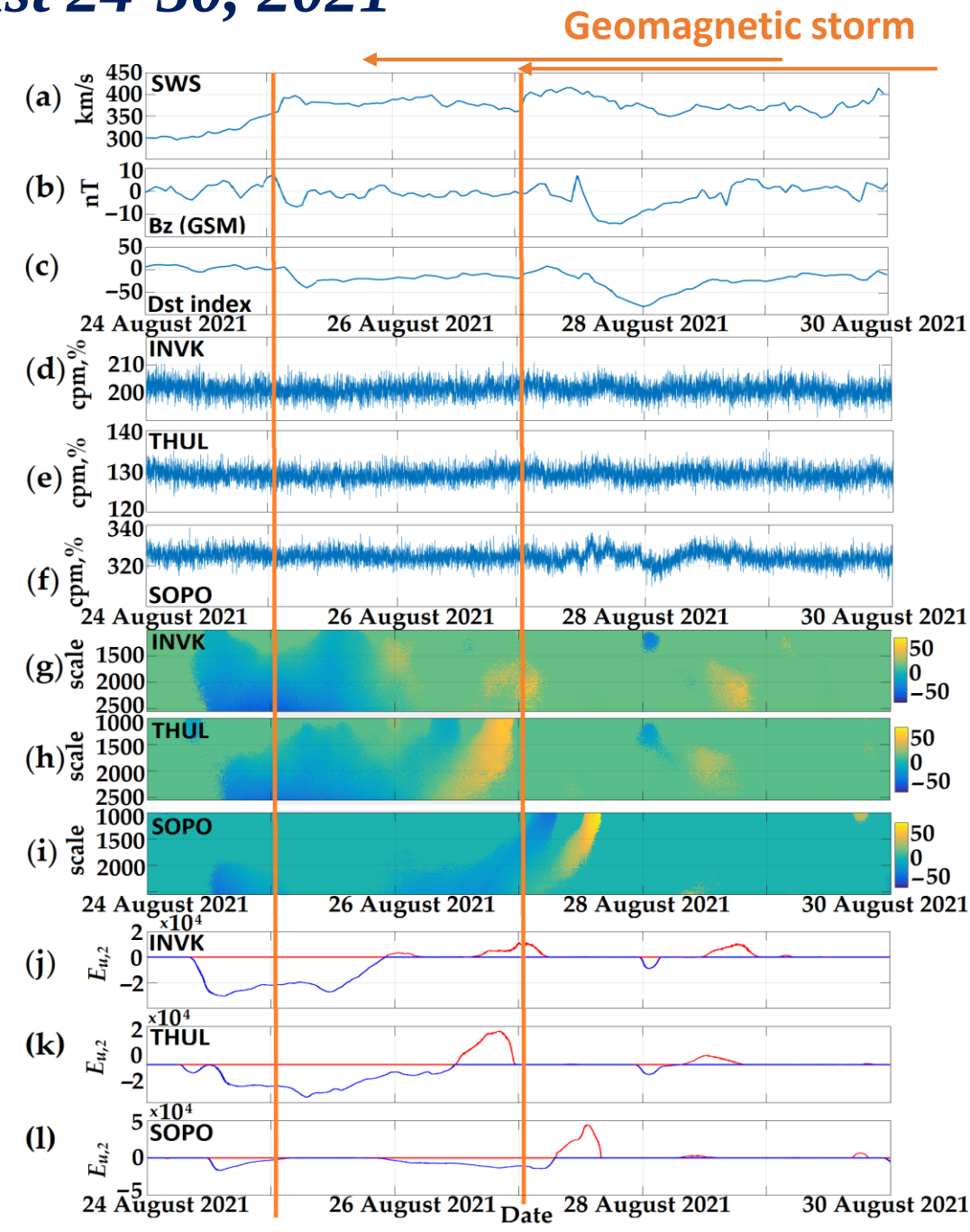

Analysis of NM data for the period May 24-30, 2019

According to the results of the method, on May 26, the intensity of cosmic rays increased at the analyzed stations. During this period, the arrival of CME was registered [http://ipg.geospace.ru].

Further, the Forbush effect was registered on May 28 at 15:00 UT. Despite the differences in the NM data from different stations, the processing results show a clearly expressed general character of the GCR dynamics. Note that the first geomagnetic disturbance (05/27/19 at 03 UT) was caused by CME, the second (05/28/19 at 19 UT) was caused by CIR, and the GCR dynamics before the events were different.

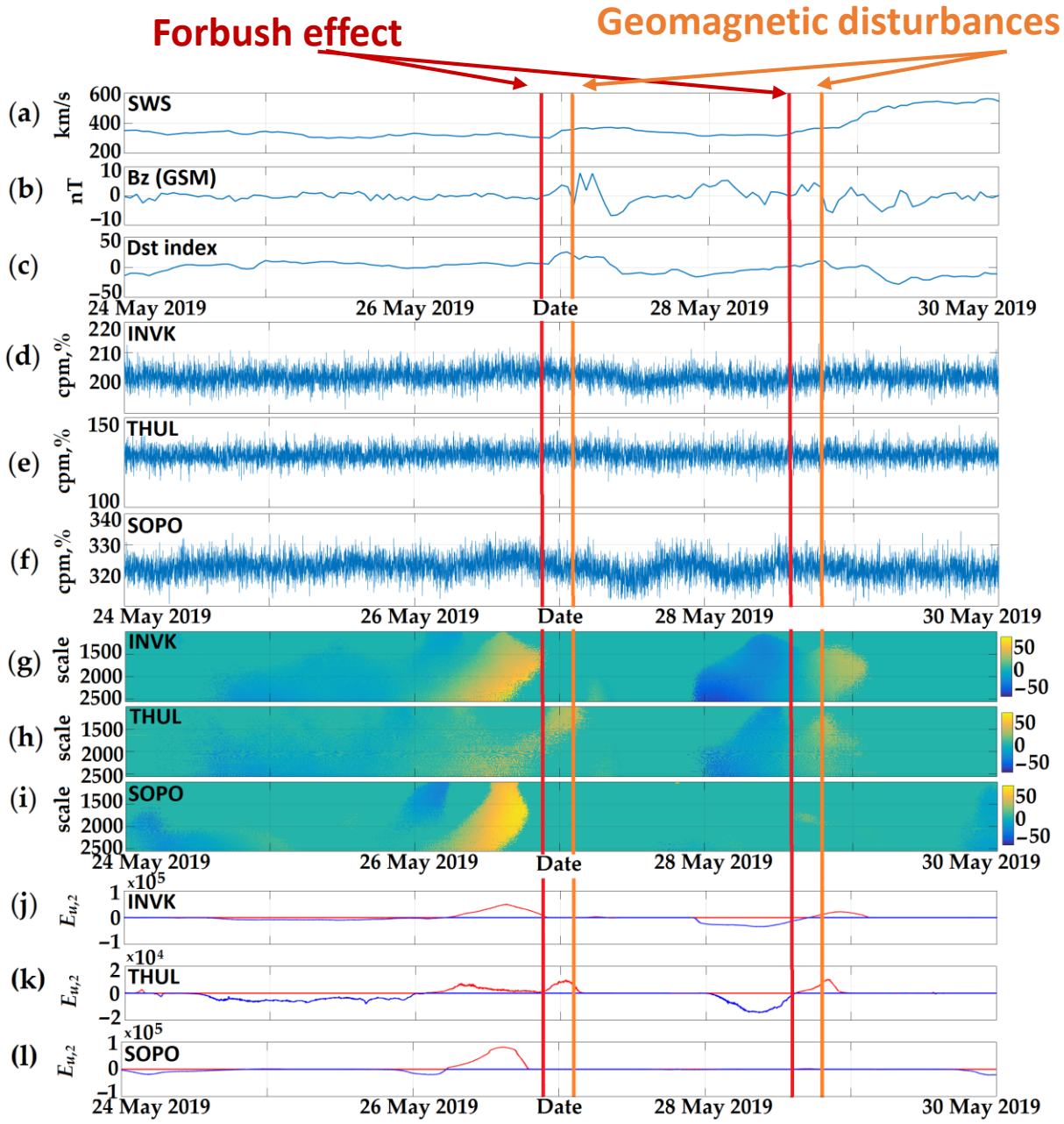

Model of the time variations of geomagnetic data

$$f(t) = \sum_{n} c_{j-m,n}\phi_{j-m,n}(t) + \sum_{b,s} P_{1,s}(W_{b,s})\,\Psi_{b,s}(t) + \sum_{b,s} P_{2,s}(W_{b,s})\,\Psi_{b,s}(t) + e(t)$$

Igor Soloviev

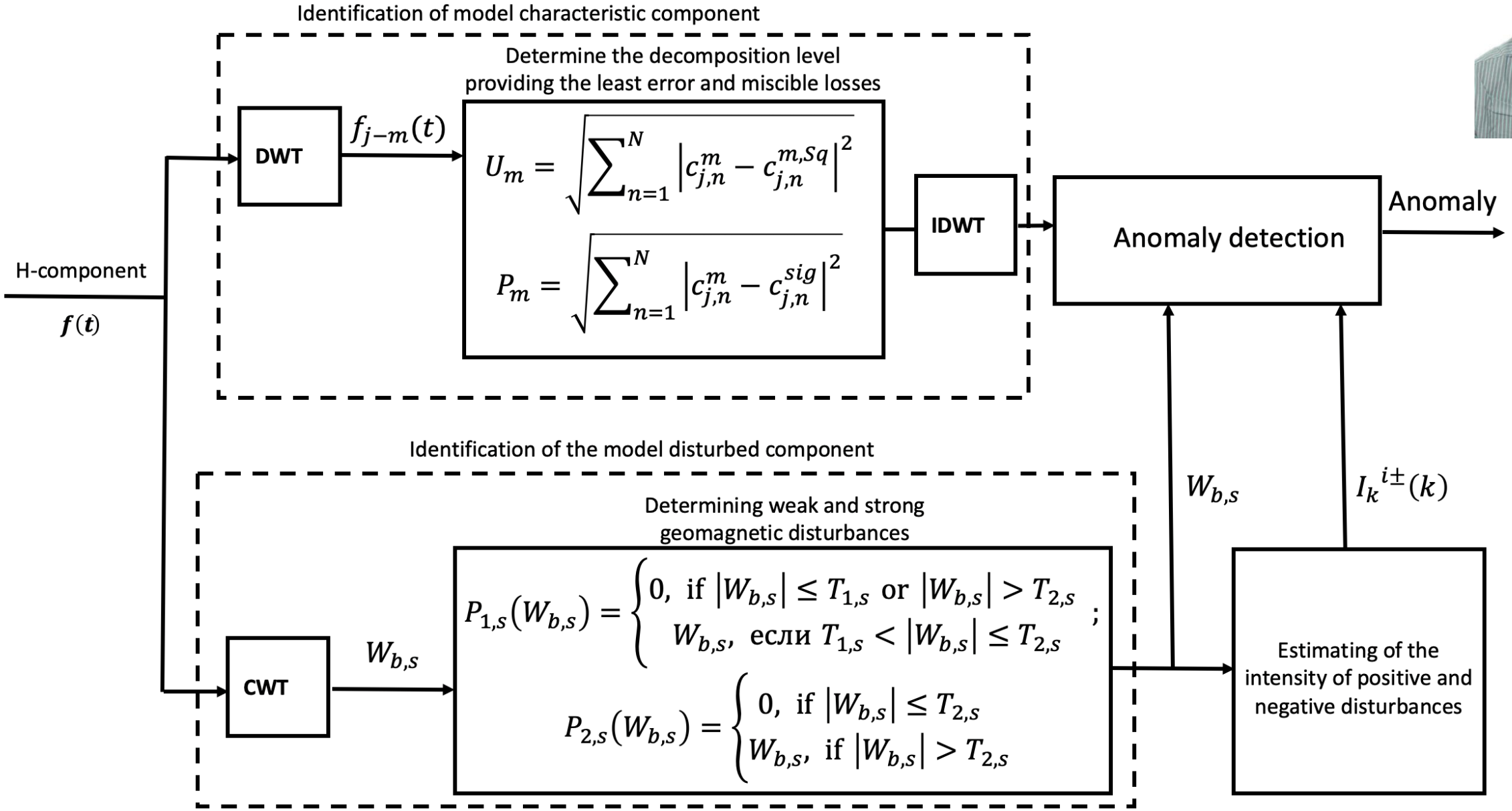

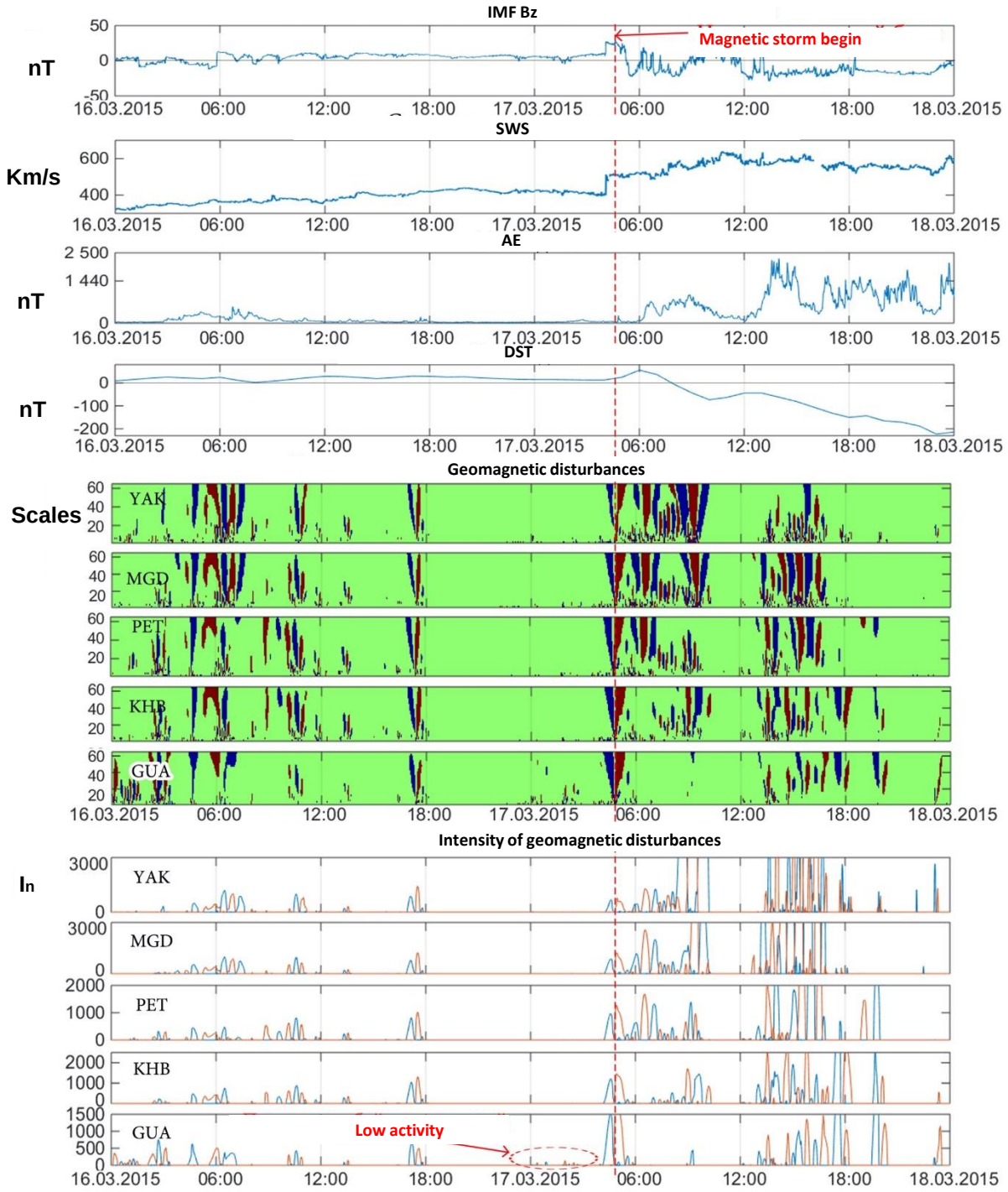

Processing of magnetic data during a strong storm on 16-17 March 2015

Before the storm, during the periods of southward fluctuations of the Bz IMF and the increase of the AE index (16 March from 02:50 to 10:00 UT), short-period weak geomagnetic disturbances occurred at the stations. The simultaneous occurrence of the disturbances at the analysed stations (from high latitudes to the equator), their essentially non-stationary nature, and their correlation with the AE index suggest that they are related to the change in the parameters of the interplanetary medium and to the increase in currents in the auroral region. At 04:00 UT on 17 March, due to the arrival of solar material from the CME, the solar wind speed increased sharply and simultaneous short-period disturbances corresponding to the sudden onset of the magnetic storm were observed at all stations. Other intense short-period disturbances were observed mainly at the more northerly stations YAK, MGD and PET.

Beginning of magnetic storm on 21 April at 15:19 UT, 2017

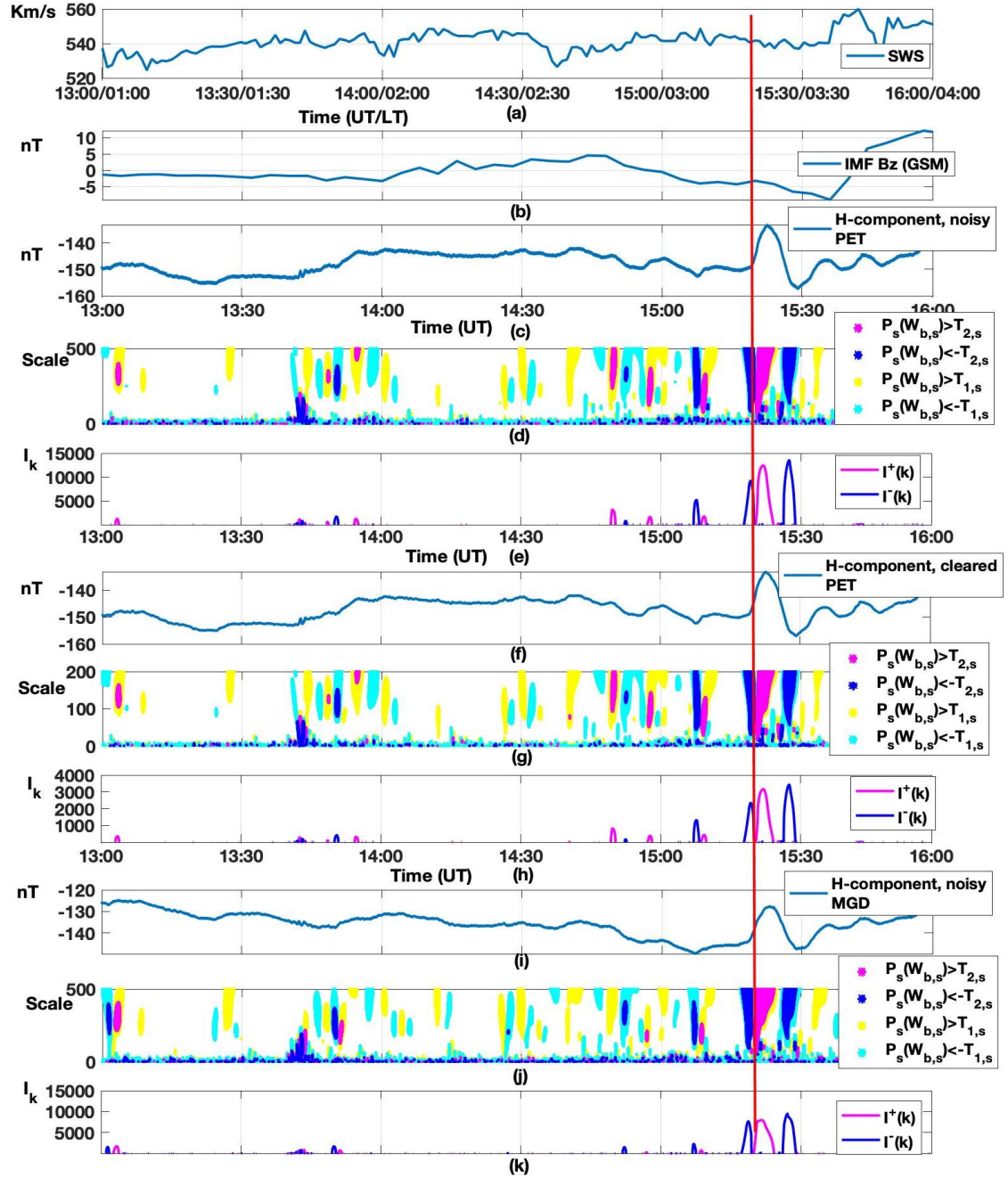

Paratunka data - the *raw* data (d, e) and *pre-processed* by the magnetologist (g, h)

The data from Magadan have not been pre-processed.

Short-period geomagnetic disturbances occur at the stations "Paratunka" and "Magadan" on the eve of the event. A general dynamics of the process is observed, but at the Magadan station the perturbations have a greater amplitude, which is related to the location of the station near the auroral latitudes. As the time of the storm onset approaches, the disturbances intensify. In the period 13:45 - 14:00 UT, at the moments of the SWS increase (a) and the insignificant increase of the fluctuations of the southward IMF Bz (b), weak perturbations of the geomagnetic field are clearly visible. The comparison of the results for the raw and pre-processed data shows that the perturbations do not significantly affect the results of the method.

Moderate magnetic storm on May 12, 2021

The increase in the intensity of the disturbances as the moment of the magnetic storm onset approaches - on 12 May at 05.49 UT (accelerated flux from the coronal hole and CME, the station was in the night sector - period 00:00 - 02:00 LT). The SWS increased significantly during this period, and the IMF Bz fluctuations increased to Bz=±20 pT. A few hours before the storm, there was a sharp increase in intensity. This was probably related to the onset of the compression region. During the event, strong perturbations occur during periods of southward IMF Bz turning, the northward direction is accompanied by a decrease in perturbations.

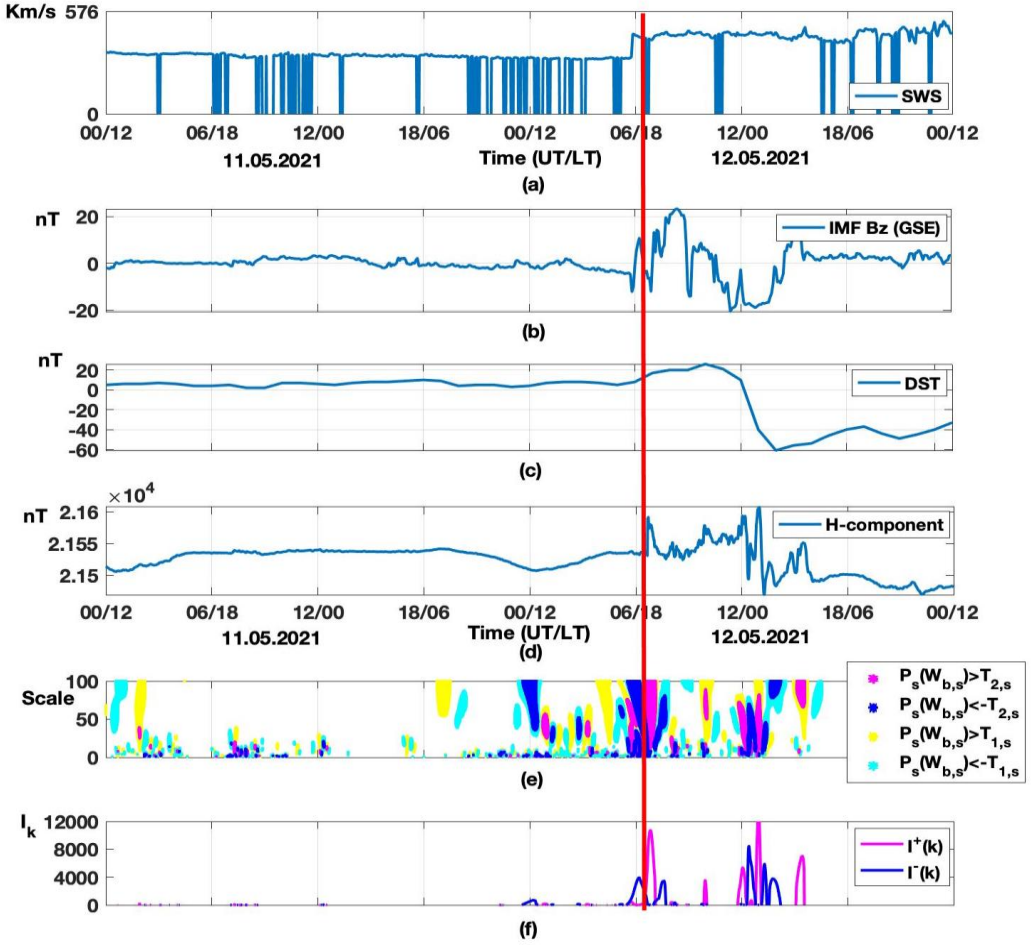

Data processing in real-time mode

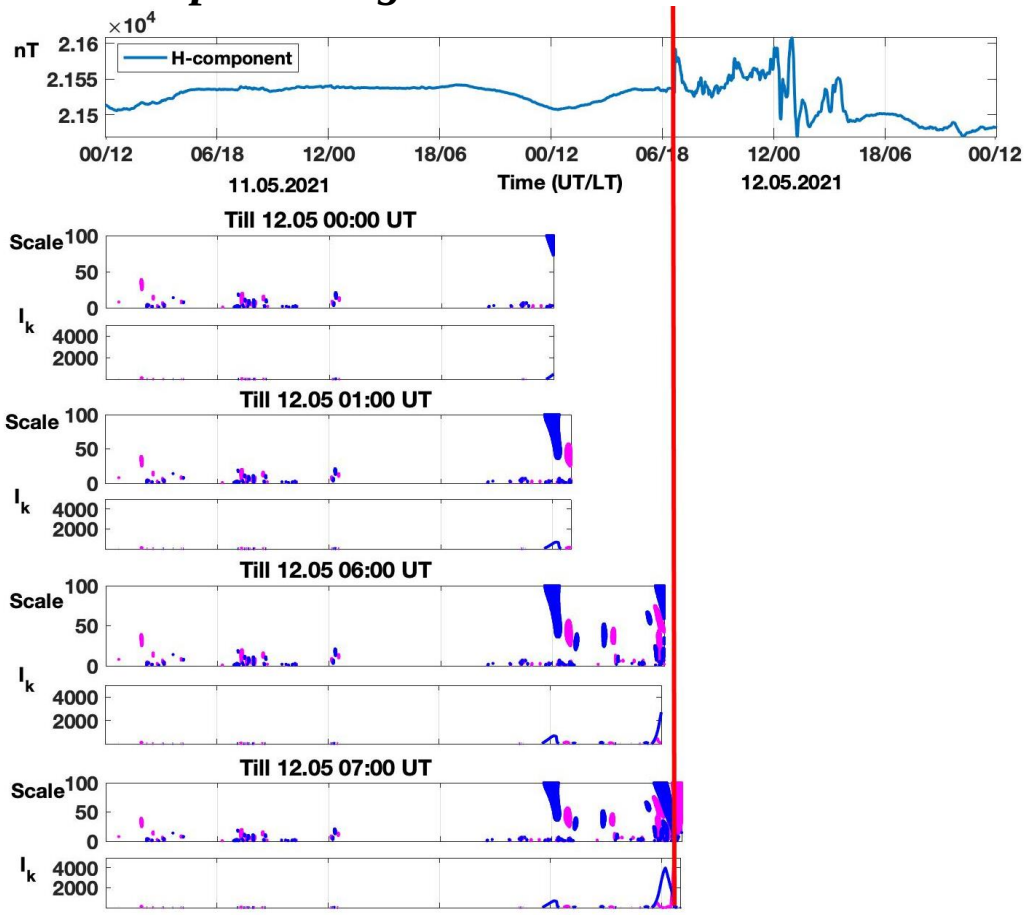

Main publications

1. Mandrikova, O.; Fetisova, N.; Polozov, Y. Hybrid Model for Time Series of Complex Structure with ARIMA Components. Mathematics **2021**, 9, 1122. https://doi.org/10.3390/math9101122.
2. Mandrikova O., Fetisova N. Modeling and analysis of ionospheric parameters based on multicomponent model // Journal of Atmospheric and Solar-Terrestrial Physics, Vol. 208, 105399, **2020**. https://doi.org/10.1016/j.jastp.2020.105399.
3. Mandrikova O, Mandrikova B, Rodomanskay A. Method of Constructing a Nonlinear Approximating Scheme of a Complex Signal: Application Pattern Recognition. Mathematics. **2021**; 9(7):737. https://doi.org/10.3390/math9070737.
4. Mandrikova, O.V., Rodomanskaya, A.I., Mandrikova, B.S. Application of the New Wavelet-Decomposition Method for the Analysis of Geomagnetic Data and Cosmic Ray Variations. Geomagn. Aeron. 61, 492–507 (**2021**). https://doi.org/10.1134/S0016793221030117.
5. Mandrikova, O.; Mandrikova, B. Method of Wavelet-Decomposition to Research Cosmic Ray Variations: Application in Space Weather. Symmetry **2021**, 13, 2313. https://doi.org/10.3390/sym13122313.
6. Mandrikova, O.; Polozov, Y.; Khomutov, S. Wavelet Model of Geomagnetic Field Variations and Its Application to Detect Short-Period Geomagnetic Anomalies. Appl. Sci. **2022**, 12, 2072. https://doi.org/10.3390/app12042072.
7. Mandrikova O, Mandrikova B. Hybrid Method for Detecting Anomalies in Cosmic ray Variations Using Neural Networks Autoencoder. Symmetry. **2022**; 14(4):744. https://doi.org/10.3390/sym14040744.
8. Mandrikova O, Mandrikova B, Esikov O. Detection of Anomalies in Natural Complicated Data Structures Based on a Hybrid Approach. *Mathematics*. 2023; 11(11):2464. https://doi.org/10.3390/math11112464
9. Mandrikova O, Polozov Y, Mandrikova B. Natural Data Analysis Method Based on Wavelet Filtering and NARX Neural Networks. *Engineering Proceedings*. 2023; 33(1):63. https://doi.org/10.3390/engproc2023033063


Thank you for your attention!